



UNIVERSITY  
OF TURKU

# STRUCTURE ELUCIDATION AND RUMINANT- RELATED BIOACTIVITIES OF PURIFIED PROANTHOCYANIDINS

---

Milla Leppä





UNIVERSITY  
OF TURKU

# **STRUCTURE ELUCIDATION AND RUMINANT-RELATED BIOACTIVITIES OF PURIFIED PROANTHOCYANIDINS**

---

Milla Leppä

## University of Turku

---

Faculty of Science and Engineering  
Department of Chemistry  
Chemistry  
The Doctoral Programme in Chemical and Physical Sciences

### Supervised by

---

Professor Dr Juha-Pekka Salminen  
Department of Chemistry,  
University of Turku, Turku, Finland

Docent Dr Maarit Karonen  
Department of Chemistry,  
University of Turku, Turku, Finland

Dr Marica Therese Engström  
Department of Chemistry,  
University of Turku, Turku, Finland

Docent Dr Petri Tähtinen  
Department of Chemistry,  
University of Turku, Turku, Finland

### Custos

---

Professor Dr Juha-Pekka Salminen  
Department of Chemistry,  
University of Turku, Turku, Finland

### Reviewed by

---

Dr Sylvain Guyot  
INRA UR1268 BIA – Polyphenols,  
Reactivity & Processes, Le Rheu,  
France

Professor Dr María Teresa Escribano-  
Bailón  
Food Science and Technology  
University of Salamanca  
Salamanca, Spain

### Opponent

---

Professor emerita Riitta Julkunen-Tiitto  
Department of Environmental and Biological Sciences  
University of Eastern Finland, Joensuu, Finland

The originality of this publication has been checked in accordance with the University of Turku quality assurance system using the Turnitin OriginalityCheck service.

ISBN 978-951-29-8273-8 (PRINT)  
ISBN 978-951-29-8274-5 (PDF)  
ISSN 0082-7002 (Print)  
ISSN 2343-3175 (Online)  
Painosalama Oy, Turku, Finland 2020

UNIVERSITY OF TURKU

The Faculty of Science and Engineering

Department of Chemistry

Chemistry

MILLA LEPPÄ: Structure elucidation and ruminant-related bioactivities of purified proanthocyanidins

Doctoral Dissertation, 168 pp.

Doctoral Programme in Physical and Chemical Sciences

November 2020

## ABSTRACT

In this thesis work, a group of natural oligomers and polymers called proanthocyanidins was studied *via* multiple chemical approaches. At first, the proanthocyanidins were purified from eleven Finnish plant species with a liquid chromatography method developed during this work. The structures of the purified proanthocyanidins were studied with mass spectrometry, which showed that the proanthocyanidins were successfully isolated from the original complex mixture of compounds into substantially simpler fractions. In the second study of this work, the bioactivities of these fractions were measured by determining their protein precipitation capacity. The results showed that the polymeric size of the proanthocyanidins was the most significant structural feature increasing their ability for protein precipitation. Other structural features were significant as well, yet their relevance to the protein precipitation capacity differed significantly amongst the tested plant species.

In the third study, the anthelmintic activities of the purified proanthocyanidins were studied *in vitro* against gastrointestinal parasite *Ascaris suum*. The effectiveness of these compounds was tested as migration inhibition activity and mortality. The results showed, that increasing polymeric size increased the anthelmintic activity of proanthocyanidins and clear differences were observed between the tested plant species as well. The similarities of the aforementioned results supported the hypothesis that the anthelmintic activities of proanthocyanidins could take place via their interactions with proteins.

Lastly, the impact of different ensiling procedures on the proanthocyanidin composition of *Vicia faba* was studied. The total proanthocyanidin concentration decreased after each treatment, and especially the amount of soluble proanthocyanidins decreased substantially. Possible explanations for the decrease of proanthocyanidin levels are either degradation of proanthocyanidins during the ensiling processes or their transformation into non-soluble forms.

**KEYWORDS:** *Ascaris suum*, bioactivity, faba bean, *in vitro*, liquid chromatography, mass spectrometry, mean degree of polymerisation, proanthocyanidin, protein

## TURUN YLIOPISTO

Luonnontieteiden ja tekniikan tiedekunta

Kemian laitos

Kemia

MILLA LEPPÄ: Puhdistettujen proantosyanidiinien rakennemääritys ja märehtijöihin liittyvät bioaktiivisuudet

Väitöskirja, 168 s.

Fysikaalisten ja kemiallisten tieteiden tohtoriohjelma

marraskuu 2020

### TIIVISTELMÄ

Tässä väitöskirjatyössä perehdyttiin proantosyanidiinien, tutkimukseen erilaisin kemiallisin menetelmin. Työhön valittiin 11 suomalaista kasvilajia, joista tutkittavat yhdisteet eristettiin. Aluksi proantosyanidiinit puhdistettiin tässä työssä kehitetyllä nestekromatografisella menetelmällä, mitä seurasi eristettyjen proantosyanidiinien rakenteen tarkka määrittäminen massaspektrometrian avulla. Nämä mittaukset osoittivat, että proantosyanidiinit kyettiin erottamaan toisistaan tehokkaasti alkuperäistä yhdisteseosta huomattavaksi yksinkertaisemmiksi jakeiksi. Työn toisessa osassa puhdistettujen jakeiden bioaktiivisuus määritettiin niiden proteiinsaostuskykyä mittaamalla. Tulokset osoittivat proantosyanidiinien koon olevan merkittävien rakenteellisten tekijä, joka lisäsi niiden aktiivisuutta. Myös muiden rakenteellisten ominaisuuksien todettiin olevan merkittäviä, mutta näiden vaikutuksen suuruus vaihteli merkittävästi eri kasvilajeilla.

Työn kolmannessa osassa puhdistettujen proantosyanidiinien antiloisaktiivisuutta arvioitiin *Ascaris suum* -suolistoloista vastaan *in vitro* -tutkimuksessa. Tutkimus suoritettiin tarkastelemalla, miten tehokkaasti proantosyanidiinikäsittely inhiboi loisten kulkeutumista agar-geelissä sekä, miten tehokkaasti käsittely tappoi loisia. Antiloismittausten tulokset olivat samansuuntaisia kuin proteiinsaostuskyvyn tapauksessa. Proantosyanidiinien suuren koon havaittiin olevan merkittävä aktiivisuutta lisäävä tekijä, minkä lisäksi erot aktiivisuudessa kasvilajien välillä olivat merkittäviä. Niin proteiinsaostus kuin antiloismittausten tulosten samankaltaisuus tuki hypoteesia, jonka mukaan proantosyanidiinien antiloisaktiivisuusmekanismi liittyy niiden kykyyn vuorovaikuttaa proteiinien kanssa.

Työn viimeisessä osassa tutkittiin eri säilöntämenetelmien vaikutusta härkäpavun (*Vicia faba*) proantosyanidiinipitoisuuteen ja -koostumukseen. Proantosyanidiinipitoisuus väheni kokonaisuudessaan merkittävästi kaikissa käsittelyissä, sekä erityisesti liukoisten proantosyanidiinien määrä laski merkittävästi. Mahdollisia syitä vähentyneelle proantosyanidiinipitoisuudelle olivat joko niiden hajoaminen tai muuntuminen liukenemattomaan muotoon.

ASIASANAT: *Ascaris suum*, bioaktiivisuus, härkäpapu, *in vitro*, keskimääräinen polymerisaatioaste, massaspektrometria, nestekromatografia, proantosyanidiini, proteiini

# Table of contents

<b>Table of contents</b> .....	<b>5</b>
<b>Abbreviations</b> .....	<b>7</b>
<b>List of Original Publications</b> .....	<b>9</b>
<b>1 Introduction</b> .....	<b>10</b>
1.1 Structure of proanthocyanidins .....	10
1.2 Purification of proanthocyanidins .....	11
1.2.1 Size exclusion chromatography .....	12
1.2.2 Normal- and Reversed-phase chromatography .....	12
1.2.3 Counter-current chromatography .....	13
1.3 Analysis of proanthocyanidins .....	14
1.3.1 Fundamental concepts of mass spectrometry .....	14
1.3.2 Fragmentation .....	15
1.3.3 Characterisation .....	16
1.4 Bioactivity of proanthocyanidins .....	18
1.4.1 Protein binding and precipitation .....	19
1.4.2 Anthelmintic activity .....	20
1.4.3 Bioavailability .....	22
<b>2 Materials and Methods</b> .....	<b>24</b>
2.1 Isolation and purification of proanthocyanidins .....	24
2.1.1 Extraction .....	24
2.1.2 Sephadex LH-20 fractionation .....	25
2.1.3 Semipreparative purification .....	26
2.2 Mass spectrometric analysis .....	27
2.2.1 UPLC-DAD-QqQ .....	27
2.2.2 UPLC-DAD-Q-Orbitrap .....	28
2.3 Turbidimetric assay .....	29
2.4 <i>Ascaris suum</i> <i>in vitro</i> assay .....	29
2.4.1 Proanthocyanidin samples .....	29
2.4.2 Nematodes .....	29
2.4.3 Migration inhibition and mortality assay .....	30
2.5 Statistical methods .....	30
<b>3 Results and discussion</b> .....	<b>31</b>
3.1 Semipreparative purification of proanthocyanidins .....	31
3.2 Proanthocyanidin composition of semipreparative fractions ...	32
3.2.1 UPLC-DAD-QqQ .....	32

3.2.2	UPLC-DAD-Q-Orbitrap.....	35
3.3	Protein precipitation capacity of proanthocyanidins.....	39
3.3.1	Effect of structural features and retention time.....	39
3.3.2	Fraction by fraction comparison of <i>Ribes alpinum</i> .....	45
3.4	Anthelmintic activity of proanthocyanidins.....	46
3.4.1	Effect of structural features and retention time.....	46
3.4.2	Plant-by-plant comparison.....	47
3.4.3	Linkage between protein precipitation capacity and anthelmintic activity.....	49
3.5	Ensiling of <i>Vicia faba</i> .....	50
<b>4</b>	<b>Conclusions.....</b>	<b>52</b>
	<b>Acknowledgements.....</b>	<b>54</b>
	<b>References.....</b>	<b>57</b>
	<b>Original Publications.....</b>	<b>65</b>

# Abbreviations

BSA	Bovine serum albumin
CCA	Concentration corrected abundance
CCC	Counter current chromatography
CID	Collision induced fragmentation
CT	Condensed tannin
DAD	Diode array detector
DM	Dry matter
DMSO	Dimethyl sulfoxide
DP	Degree of polymerisation
EG	Estimated galloyl content in relation to proanthocyanidin content
EIC	Extracted ion chromatogram
ESI	Electrospray ionisation
ex	Extension unit
GIN	Gastrointestinal nematode
HBSS	Hank's balanced salt solution
HRF	Heterocyclic ring fission
HRMS	High-resolution mass spectrometry
HT	Hydrolysable tannin
IA-%	Percentage of inhibition activity
LC	Liquid chromatography
MALDI	Matrix assisted laser desorption ionisation
mDP	Mean degree of polymerisation
<i>m/z</i>	Mass-to-charge ratio
MRM	Multiple reaction monitoring
MS	Mass spectrometry
$M_w$	Molecular weight
NP	Normal-phase chromatography
PA	Proanthocyanidin
PC	Procyanidin
PD	Prodelphinidin
PD-%	Proportion of prodelphinidin

PLSR	Partial least squares regression
PPC	Protein precipitation capacity
Q	Quadrupole
QM	Quinone methide
QqQ	Triple quadrupole
RDA	Retro-Diels–Alder
RP	Reversed-phase chromatography
RPMI	Roswell Park Memorial Institute
SEC	Size-exclusion chromatography
SRM	Single reaction monitoring
ter	Terminal unit
$t_R$	Retention time
TOF	Time-of-flight
UPLC	Ultra high-performance liquid chromatography
WFI	Water for injection

# List of Original Publications

This thesis is based on the following publications and additional unpublished results. The publications are referred in the text by their Roman numerals **I–IV**.

- I** Leppä, M. M., Karonen, M., Tähtinen, P., Engström, M. T., and Salminen, J.-P., Purification of chemically well-defined semipreparative liquid chromatography fractions from complex mixtures of proanthocyanidin oligomers and polymers, *Journal of Chromatography A*, 2018, 1576:67–79, <https://doi.org/10.1016/j.chroma.2018.09.034>
- II** Leppä, M. M., Laitila, J. E., and Salminen, J.-P., Distribution of protein precipitation capacity within variable proanthocyanidin fingerprints, *Molecules*, 2020, 25(21): 5002, <https://doi.org/10.3390/molecules25215002>
- III** Leppä M. M., Williams A. R., Karonen M., Tähtinen P., Engström M. T., and Salminen J.-P., Anthelmintic activity of refined proanthocyanidin fractions against *Ascaris suum*, to be submitted to *Phytochemistry*, 2020.
- IV** Rinne M., Leppä M. M., Kuoppala K., Koivunen E., Kahala M., Jalava T., Salminen J.-P., and Manni K., Fermentation quality of ensiled crimped faba beans using different additives with special attention to changes in bioactive compounds, *Animal Feed Science and Technology*, 2020, 265, 114497, <https://doi.org/10.1016/j.anifeedsci.2020.114497>.

Article **I**, copyright © 2018 Elsevier, reprinted with permission.

Article **II**, copyright © 2020 MDPI, published under an open access Creative Common CC BY license.

Article **IV**, copyright © 2020 Elsevier, reprinted with permission.

# 1 Introduction

## 1.1 Structure of proanthocyanidins

Proanthocyanidins (PAs) form a diverse group of compounds, which all are composed of rather similar building blocks. The basic structure of a flavan-3-ol consists of flavan backbone with hydroxylation in the C-3,5 and 7 positions.<sup>1,2</sup> The flavan-3-ol unit (Figure 1) can appear in several different forms depending on the hydroxylation degree of the B ring, orientation of the B ring and OH group of the C-3 position (*cis* or *trans*) and possible conjugates in the C-3 position. The *cis* configuration is indicated with *epi*-prefix in the naming of the compounds. The flavan-3-ol with monohydroxylated B ring is called (epi)afzelechin, dihydroxylated (epi)catechin and trihydroxylated (epi)galocatechin.

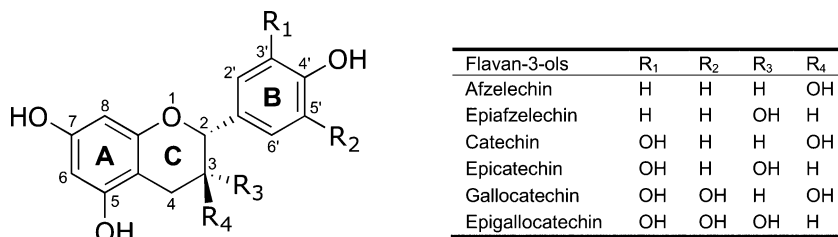


**Figure 1.** The structure of monomeric flavan-3-ol with different hydroxylation degrees in the B ring.

The monomer units are linked to each other via interflavan linkages (Figure 2). B-type linkage refers to a single covalent carbon-carbon bond between the structural units, such as C4-C8 or C4-C6, whereas A-type linkage refers to the structures with an additional C2-O7 or C2-O5 bond between the flavan-3-ols.<sup>3</sup> Additional conjugates can be a part of PA structure and the most common conjugation type is the galloylation of O-3 position.<sup>4</sup> The number of galloyl groups per single PA molecule is called the degree of galloylation.

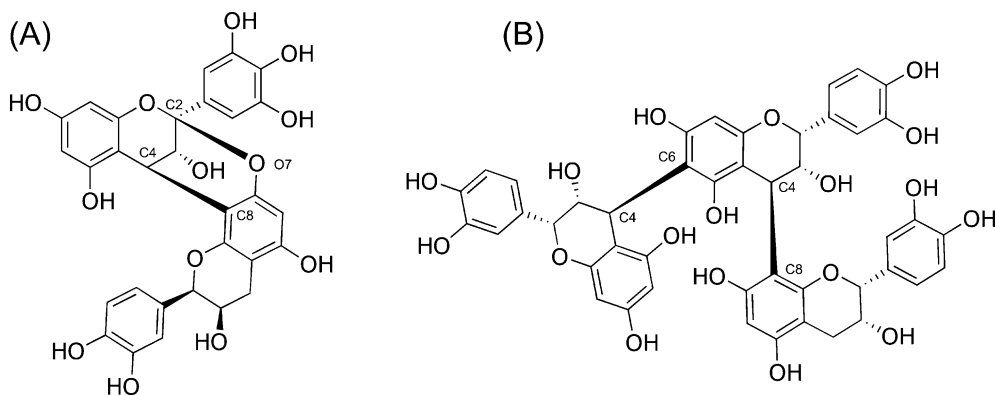


**Figure 2.** Schematic (A) dimeric prodanthocyanidin with C4—C8 B-type and C2—O7 A-type interflavan linkages and (B) trimeric branched proanthocyanidin with C4—C6 and C4—C8 B-type interflavan linkages.

The hydroxylation degree of the B ring in the monomeric building blocks gives basis to the names of the PA structural units. Propelargonidins contain monogalloylated (OH in C4'), procyanidins (PCs) digalloylated (OH in C3' and C4') and prodelfinidins (PDs) trigalloylated B ring (OH in C3', C4' and C5').<sup>5</sup> The most common structural units are PCs and PDs, both of which can be present in a same PA molecule. Depending on the relative ratio of the PC and PD of the complete PA mixture, the PAs can be described either as PC or PD rich PAs.

The sizes of individual PA molecules can vary from small dimers up to very large polymers including tens of monomeric flavan-3-ol units. In this thesis, the relatively small PAs consisting of two to ten flavan-3-ol units are referred as oligomers whereas PAs with higher degree of polymerisation (DP > 10) are referred as polymers. Plants produce a diverse mixture of different PAs with different polymeric sizes and therefore the mean degree of polymerisation (mDP) is a commonly used measure for the average size of the studied PAs. Even though this measure is heavily used, it is relevant to keep in mind, that the PA composition is much more complex than the single mDP value would indicate.

## 1.2 Purification of proanthocyanidins

Chromatography is a widely used field of diverse analytical techniques, which are utilised in the analysis and purification of variety of different compounds. Different kinds of chromatographic techniques are suitable for different sample types. The mutual feature for all chromatographic approaches is the use of mobile and stationary phase, which are utilised in the elution of the sample.<sup>6</sup> The sample is introduced to the system and mobile phase runs through the stationary phase. The analytes are separated from each other based on their interaction with the both phases and their

willingness to travel with the mobile phase rather than to remain within the stationary phase. In liquid chromatography (LC)<sup>6</sup>, the stationary phase is a solid material and liquids are utilised as mobile phases. In counter current chromatography (CCC) two immiscible liquids are utilised as mobile and stationary phase.<sup>7</sup>

Different chromatographic methods are classified based on the mechanism of separation. In size-exclusion chromatography (SEC) the analytes are separated based on their size and in normal- or reversed-phase (NP or RP) chromatography the separation takes place due to the difference in polarity between the mobile and stationary phase. In the isolation and purification of PAs, it is often necessary to combine multiple fractionation steps and methods to obtain the desired compounds.<sup>8</sup>

### 1.2.1 Size exclusion chromatography

The most commonly utilised size-exclusion chromatography (SEC) resins in the purification of PAs are different Sephadex<sup>8-10</sup> and Toyopearl<sup>11</sup> materials. Even though, these resins are considered as SEC materials, the mode of separation is closer to absorption than size-exclusion and the analytes are partially separated based on their affinity towards the material.<sup>12</sup> A common approach is to use these materials in step-by-step gradient elution to remove sugars and flavonoids from the column with methanol/water mixture before the elution of PAs with high acetone percentage.<sup>13,14</sup>

Multiple different approaches can be utilised in the SEC purification. For instance, they can be used as pre-purification method for the isolation of the PAs from the rest of the plant extract.<sup>15</sup> Another approach is to use the Sephadex G-25 for the separation of fractions with variable mDP.<sup>9</sup> Relatively small individual oligomers, such as dimer and trimers can be separated by SEC<sup>16</sup> and also, large amounts of facile PA fractions can be produced as well<sup>10</sup>.

### 1.2.2 Normal- and Reversed-phase chromatography

The LC techniques utilising polarity differences of mobile and stationary phases are normal-phase (NP) and reversed-phase (RP) chromatography.<sup>6</sup> In RP, the stationary phase is non-polar *e.g.* silica based material with bound alkyl chains, and the mobile phase is a polar solvent or solvent mix, usually water or mixture of water-soluble organic solvent and water. In NP systems, the stationary phase is more polar than the mobile phase, which is usually a non-polar organic solvent, such as hexane. The most commonly used approaches in the analysis and separation of PAs are NP<sup>17,18</sup> and RP<sup>19,20</sup> chromatographic methods.

The NP chromatography is able to separate the PAs by their polymeric size up to decamer<sup>17</sup> whereas the RP is unable to separate the large oligomers or polymers.

The separation of even up to DP of 14 has been reported utilising diol column.<sup>21</sup> The combination of normal- and reversed-phase LC has been utilised in the purification and analysis of dimeric PAs.<sup>19</sup> For instance, Appeldoorn et al.<sup>18</sup> firstly isolated the dimer mixture with NP and then separated all the dimers from each other via RP ending up with six PC dimers including A- and B-type PAs.

Preparative or semipreparative RP or NP purification of PAs is usually carried out with pre-purified or fractionated PA material.<sup>15,18</sup> Sephadex fractionation is a relatively common pre-step before RP fractionation<sup>15</sup> and even the RP fractionation as such can be repeated to result in the desired separation.<sup>20</sup>

### 1.2.3 Counter-current chromatography

Counter-current chromatography (CCC) is a chromatographic technique, which utilises two immiscible liquids in the separation of analytes.<sup>22</sup> The stationary phase is held in place with the help of centrifugal force and the mobile phase is pushed through the stationary phase. When the centrifugal force is applied to the coil, which functions as a column the higher density liquid occupies the other end called the tail and the lower density liquid occupies the other end called the head. The CCC system can be operated in the normal- or reversed-phase mode depending on the selection of mobile and stationary phases and whether the mobile phase is pumped from tail to head or head to tail. The analytes are separated based on their differences in polarity. The number of different possible combinations of eluents is vast and the proper selection of eluents is crucial for the performance of the separation.<sup>23</sup>

The use of two liquid phases instead of a solid stationary phase eliminates any potential irreversible absorption of the sample material to the stationary phase, and thus, enables the full recovery of analytes.<sup>7,8</sup> The use of fresh solvents in each purification run, removes the need for pre-purification steps in the case of CCC, thus even crude extracts can be purified with CCC.<sup>24</sup> There are many examples in utilising the CCC in the purification of PAs.<sup>25</sup> The smaller oligomers, such as dimers can be individually separated<sup>26</sup> and larger oligomers up to pentamers can be separated based on their DP as well<sup>27</sup>.

## 1.3 Analysis of proanthocyanidins

### 1.3.1 Fundamental concepts of mass spectrometry

#### Ionisation techniques

In mass spectrometry (MS), the analytes are detected as negative or positive ions and the mass-to-charge ratio ( $m/z$ ) of the analytes is recorded. Prior to the analysis, the analysed molecules are brought to gas phase and ionised. One of the most common ionisation techniques in the modern-day mass analysis of natural products is electrospray ionisation (ESI).<sup>28,29</sup> ESI is considered as a soft ionisation technique, which means that the majority of analytes stay unfragmented during the ionisation and they are analysed as singly or multiply charged non-fragmented ions. Obviously, fragmentation can occur as well depending on the source conditions. By controlling the source parameters, even extensive fragmentation can be achieved with high cone voltage.<sup>29,30</sup>

Matrix assisted laser desorption ionisation (MALDI) is also a commonly used ionisation technique, which produces intact ions. In this ionisation technique, the analytes are firstly absorbed in the matrix material, where they are eventually brought to gas phase and ionised *via* laser beam.<sup>31</sup> MALDI is a popular ionisation technique in the analysis of large analytes, such as high DP PAs<sup>32</sup> and PA–protein complexes<sup>33–35</sup>.

#### Mass analysers

Different mass analysers serve different functions. While some analysers are more suited in detailed structural analysis due to their high-resolution, some analysers are more fitted in quantitative analysis from trace level analyte concentration. One of the most useful instruments in the quantitative analysis of PAs is highly sensitive triple quadrupole (QqQ) instrument, which Engström et al<sup>29</sup> utilised in group specific quantitation of PC and PD units. Also, ion trap analysers can be utilised in tandem-MS mode.<sup>17,36</sup> Common instruments in accurate structural analysis are for instance, orbitrap<sup>3</sup> and quadrupole time-of-flight (QTOF)<sup>37</sup> analysers, which are considered as high-resolution mass spectrometric (HRMS) instruments.

ESI is a versatile ionisation source, which can be coupled to nearly any kind of mass analyser. It is often coupled to quadrupole (Q)<sup>28</sup> or QqQ<sup>29</sup> instrument, when utilised in PA analysis. It is also suitable to be connected with high-resolution ion trap<sup>3,38</sup> and TOF<sup>39</sup> instruments. Since, the detection range of these analysers can be lower than the masses of the PAs with high DP, the multiply charged ions from the ESI source extend the detection range of large polymeric PAs. MALDI is often

coupled to TOF or QTOF mass analysers due to their broader detection area, and the analytes are detected as singly charged ions.<sup>32,33</sup>

### Tandem mass spectrometry

The tandem mass (MS/MS) analysis can occur either in time or in space. The number of consecutive MS analyses per ion can be pointed out with a superscript (MS<sup>n</sup>). An example of an in space MS/MS analyser is QqQ, where the quadrupoles are located in line with each other and the separation of ions occurs with physically separate elements. In the in time tandem analysis, the separation is achieved over time within the same space. For instance, a quadrupole ion trap can perform in time tandem analyses. Tandem mass spectrometry enables the detection of precursor and product ions separately. There are multiple modes in which the tandem MS instrument can be operated. The mass analysers can either be locked to detect a single pre-set value or they can scan an *m/z* area. Such MS analysis, where the *m/z* values of both the precursor and the product ions have been pre-set, the analysis mode is called either single or multiple reaction monitoring (SRM and MRM) depending on the number of product ions. In SRM, only one precursor–product ion pair is monitored while in MRM multiple transitions are monitored at once. In daughter scan mode, the precursor ion is selected at the first mass analyser, then it is fragmented, and finally all product ions are recorded.<sup>40</sup>

The first fragmentation in MS<sup>n</sup> can occur prior analyser in the ionisation source. In this manner, the desired fragmentation products from the ionisation source can be utilised as precursor ions and the fragmentation in the collision chamber produces fragments of fragments as was carried out by Engström et al.<sup>29</sup>

### 1.3.2 Fragmentation

In addition to the formation of singly and multiply charged ions, there are typical fragmentation patterns in the MS analysis of PAs (Figure 3). In quinone-methide (QM) fragmentation, the cleavage of flavan-3-ol units produces different *m/z* values for the extension (ex) and terminal (ter) units. This enables the quantitation of extension and terminal units separately and even the estimation of the mDP.<sup>29,41</sup> In negative ionisation mode, the fragmentation of a B-type PA produces fragments at *m/z* 287 (PC<sub>ex</sub>), 289 (PC<sub>ter</sub>), 303 (PD<sub>ex</sub>), and 305 (PD<sub>ter</sub>). Another typical fragmentation pattern is retro-Diels–Alder (RDA) fragmentation, where the cleavage of a B ring occurs via the retro-Diels–Alder mechanism. Neutral losses of 136, 152, and 168 Da indicate, that the B ring was either mono-, di-, or trihydroxylated, respectively.<sup>17,36</sup> In heterocyclic ring fission (HRF), a neutral loss of 126 Da is observed as compared to the [M–H]<sup>–</sup> ion.

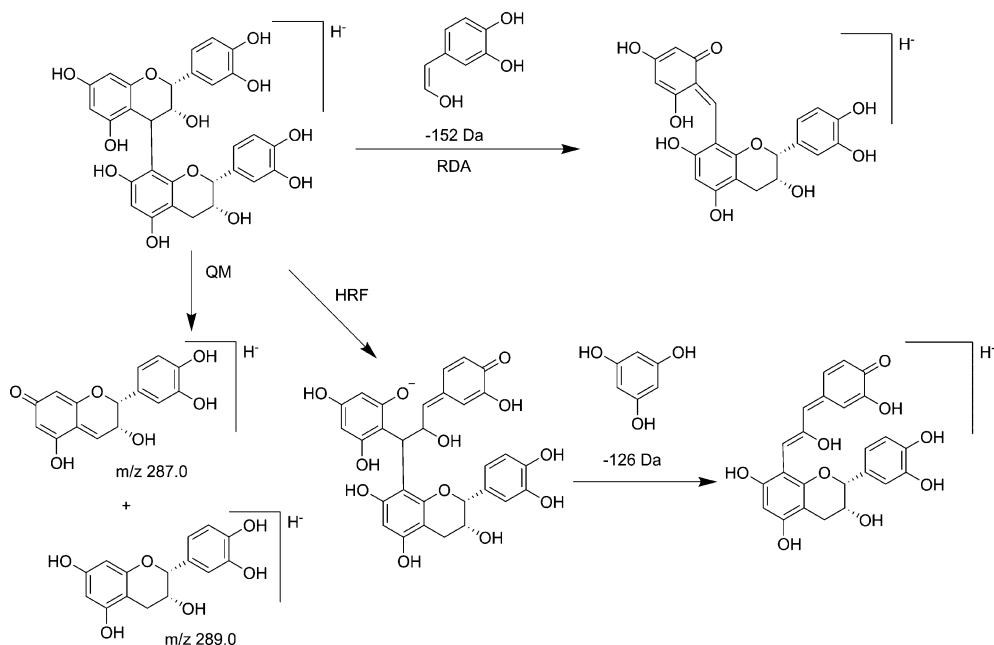


**Figure 3.** The fragmentation patterns of B-type proanthocyanidins.<sup>17,36</sup> The abbreviations are as follows: HRF, heterocyclic ring fission; QM, quinone methide cleavage and RDA, retro-Diels–Alder.

### 1.3.3 Characterisation

The determination of the molecular formula of PAs with the HRMS instruments is carried out based on isotopic patterns of the analysed ions. The isotopic patterns reveal the charge states of the ions thus enabling the accurate characterization of the molecular masses.<sup>19,28</sup> The mass spectrometric analysis of PAs with high DP relies on the multiply charged ions in the mass analysis. The multiply charged ions enable the detection of PAs with high DP with accurate detectors for which the  $m/z$  range is usually lower than the molecular weight of the PAs (Figure 4).<sup>3,39</sup> PA oligomers can be detected by their doubly to four-fold charged ions up to DP of 26 with ESI-MS.<sup>39</sup>

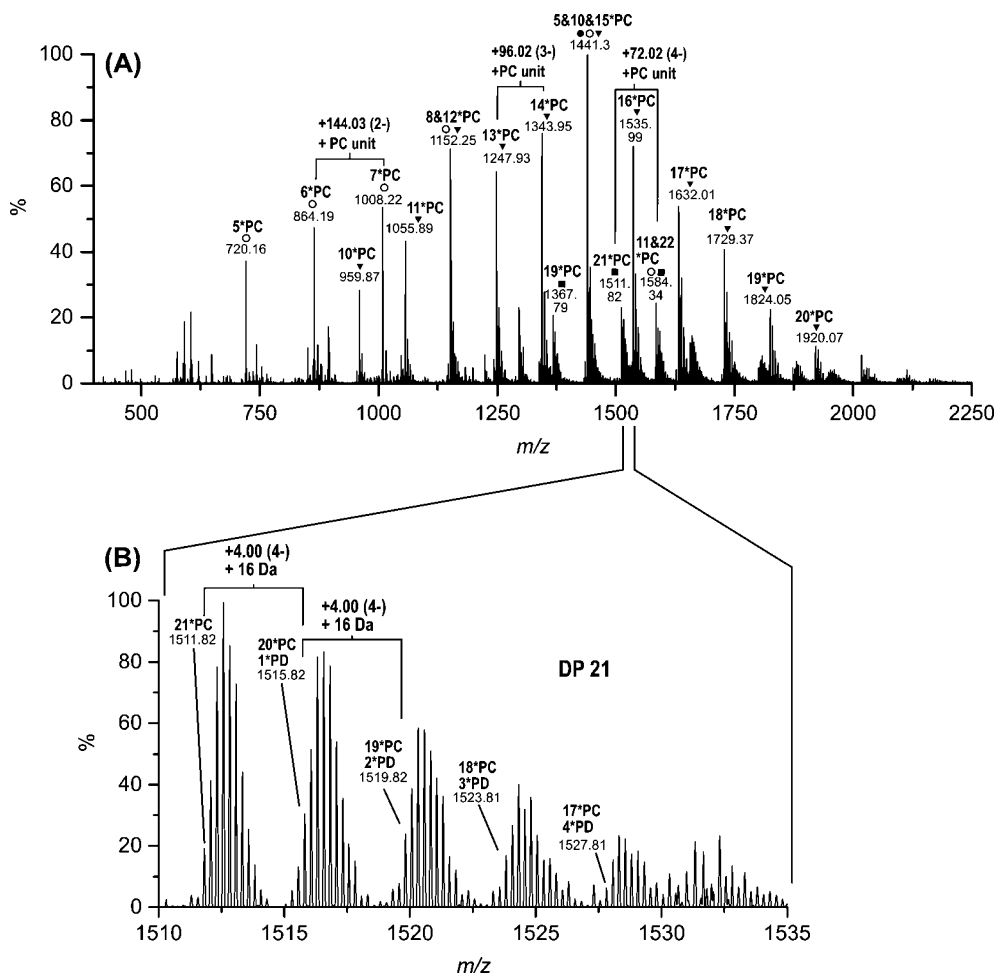


**Figure 4.** The series of signals caused by different oligomeric sizes and hydroxylation degrees of different proanthocyanidins (PAs) in high-resolution mass spectra. (A) The increments of procyanidin (PC) B-type PAs as the degree of polymerisation (DP) increases. (B) The addition of 16 Da as the hydroxylation degree of the PA structural units increase. Figure adapted from Leppä *et al* (I).

Since the PA oligomers and polymers isolated from a natural source usually contain a disperse mixture of PA molecules, the high-resolution mass spectra of the PAs exhibit as series of PA oligomers (Figure 4).<sup>32,42</sup> The singly charged series of oligomeric B-type PCs is observed at  $m/z$   $577.13 + 288.06 \times n$  ( $DP \geq 2$ ).<sup>42,43</sup> Similarly, doubly charged series of B-type PCs is found at  $m/z$   $576.13 + 144.03 \times n$  ( $DP \geq 4$ ), and triply charged series at  $m/z$   $959.87 + 96.02 \times n$  ( $DP \geq 9$ ), respectively. The B-type PAs consisting of only PD units are similarly observed as singly charged series of  $609.12 + 304.06 \times n$  ( $DP \geq 2$ ), doubly charged series of  $[M-2H]^{2-} 608.12 + 152.03 \times n$  ( $DP \geq 4$ ), and triply charged series of  $1013.19 + 101.35 \times n$  ( $DP \geq 9$ ). The disperse

nature of PAs extends the structural variation even within a single polymeric size. An increment of  $m/z$  16.00 for singly, 8.00 for doubly, 5.33 for triply and 4.00 for four-fold charged ions illustrates the increase in the hydroxylation degree within fixed polymer size.

In addition to the exact mass, even the location of an A-type bond can be deduced from the fragmentation patterns of PAs.<sup>3</sup> The QM fragments reveal whether or not the A-type bond is located between the extension and terminal units or between two extension units. Lin et al.<sup>3</sup> compared computational and experimental masses of several PAs to finally identify nearly 250 PA oligomers. The locations of A-type bonds were concluded from the fragmentation patterns in MS<sup>n</sup>.

There are multiple attempts to utilise MS in the assessment of mDP of PAs. The direct estimation of mDP from the ESI-MS data can lead to the significant underestimation of the mDP of the studied PA mixture.<sup>39</sup> This is due to the PAs with the highest DP not being visible in the ESI mass spectra. The conventional approach in the estimation of the mDP, is the depolymerisation of PAs prior analysis via acidic conditions accompanied by a nucleophilic agent such as phloroglucinol<sup>44</sup> or thiol<sup>45</sup>. The depolymerisation products are then analysed via LC-MS and the extension and terminal units are quantified separately.<sup>45</sup> An exceptional approach, which does not require the depolymerisation of the PAs prior analysis was introduced by Engström et al.<sup>29</sup> They utilised UPLC-MS/MS combined with in-source QM fragmentation<sup>17</sup> to detect the terminal extension units of PCs and PDs and collision induced dissociation (CID) to verify the detection of these units via PC and PD specific fragmentation.<sup>29</sup>

## 1.4 Bioactivity of proanthocyanidins

PAs are a group of highly bioactive plant specialised metabolites. Their bioactivity becomes evident in multiple forms. For instance in agriculture, PA rich feeds have been witnessed to lower the burden of gastrointestinal nematodes (GIN) in ruminants<sup>46</sup>, improve the quality of milk<sup>47</sup> and meat<sup>48,49</sup> and lower the methane emissions from the rumen<sup>50</sup>. The mechanisms of the aforementioned favourable effects are not yet fully resolved, but certain characteristic features of PAs have been observed to play the key role for the activity. Also, certain chemical activities such as protein precipitation capacity (PPC) and oxidative activity may predict some other forms of bioactivity such as anthelmintic activity. This linkage has been studied in more detail in the case of HTs.<sup>51</sup>

### 1.4.1 Protein binding and precipitation

The interactions between PAs and protein have been extensively studied for decades via multiple different experimental approaches.<sup>52–57</sup> Hydrophobic interaction<sup>52,54,58</sup>, hydrogen bonding and aromatic stacking<sup>59</sup> play an important role in the complex formation between PAs and proteins. The hydrophobic interaction has been proposed to be the dominant mode of interaction<sup>54,58,60</sup>, whilst the hydrogen bonding can be the secondary mode of interaction. These non-covalent interactions lead to the formation of non-covalent PA–protein complexes which can take either soluble or insoluble forms depending on the relative concentrations of the PA and the protein.<sup>61</sup>

The complex formation is strongly affected by the structure of the PA<sup>55,57,62</sup> and the protein<sup>63</sup> as well as their concentrations and ratio in the solution<sup>62,64</sup>. Also, the reaction conditions such as pH<sup>65,66</sup>, ionic strength<sup>64</sup> and solvent composition<sup>58</sup> affect the reaction. The formation of non-covalent PA–protein complexes is favoured at a pH which is near the isoelectric point of the protein.<sup>66</sup> In the case of bovine serum albumin (BSA), the optimal pH is at 4.5–5.0.<sup>65</sup>

The PA–protein complexation consists of multiple steps including the coating of the surface of the protein by the PA molecules, the formation of cross-linkages and eventually precipitation.<sup>59,61</sup> This means, that not all of the formed complexes are insoluble, but the amount of insoluble complexes depends on how actively the soluble complexes crosslink to each other forming the insoluble complex network. Few mechanisms for the formation of the cross-linkages have been proposed, some of which suggest that the network of PA–protein complexes is formed based on  $\pi$ – $\pi$  stacking of the aromatic rings<sup>59</sup> whereas another study suggests that the hydroxyl groups of the PAs form linkages via hydrogen bonding<sup>61</sup>.

Due to the different conceptions of the complex formation mechanism, the importance of certain structural features of the PAs has been emphasised. The number of hydroxyl groups and the molecular size are clearly key functional factors in the PA–protein complexation. Many studies have shown that high DP or mDP increases the affinity of PAs towards proteins<sup>67</sup> and also the formation of insoluble PA–complexes.<sup>56,57,68,69</sup> In addition, the possible galloylation of flavan-3-ol units offers an extra binding site enhancing the level of complexation as compared to the non-galloylated flavan-3-ol units.<sup>62,70</sup> In PD units, the additional hydroxyl group of the B ring should increase the probability of hydrogen bonding between the PA and protein and thus, improve the protein precipitation.<sup>61</sup> Yet the experimental proof of elevated protein precipitation with higher PD proportions has been inconsistent.<sup>57,71</sup>

From the hydrophobicity point of view, A-type bonding has been observed to favour the precipitation.<sup>60</sup> The presence of an A-type bond increases the rigidity of a PA molecule<sup>72</sup>, and also, eliminates one hydroxyl group from the PA structure<sup>1</sup> increasing the hydrophobicity of the molecule. The increased hydrophobicity may

ultimately favour the complex formation more than the presence of hydroxyl groups, thus increasing protein binding and eventually precipitation. Also, the 3D structure of the PA structural units plays a key role in the precipitation. Cala et al.<sup>59</sup> compared the PA–protein precipitation of PC dimers (B1, B2, B3, and B4) and a trimer (C2) and discovered that those PAs which did not favour intramolecular  $\pi$ – $\pi$  stacking precipitated proline-rich protein more effectively.

Insoluble complexes are visible and their amount in solution can be measured rather simply by observing the haze formation in the solution. The experimental design utilising the passage of light in the colloidal liquid is called turbidimetry.<sup>73</sup> In turbidimetry, the elevated absorbance of light due to the higher amount of particles in the solution is measured. The loss of intensity of a light beam ( $\lambda = 290$ – $410$  nm) with a pre-set wavelength is measured as the light passes through a cuvette and the transmitted light is detected. Previously, the turbidimetric approach has been utilised in the complexation of both the HTs<sup>51,74</sup> and the PAs<sup>57</sup>.

#### 1.4.2 Anthelmintic activity

The drug-resistance of GINs has been increasing at an alarming rate during the last 10 to 15 years. It is one of the most urgent threats of the modern-day agriculture<sup>75</sup> causing massive economic losses<sup>76</sup>. Anthelmintic effects of PA rich plant species has been witnessed by several researchers worldwide<sup>77,78</sup> thus, the research interest towards tanniferous plants as parasitic controlling agents has increased substantially in the last decade.<sup>78–80</sup> The potential anthelmintic activity of these plants has led to the suggestion of using these plants as nutraceuticals<sup>81,82</sup> for treating the parasitic infections instead of synthetic drugs. PAs are particularly abundant in multiple plant species, which have been utilised as feeds or forage, such as Alfalfa, Sainfoin, *Lotus*, Lespedeza and clovers.<sup>78,83</sup> The anthelmintic activity of these plants has been considered to originate from the condensed and/or hydrolysable tannins.<sup>83</sup>

The anthelmintic assays can target different stages in the life cycle of the parasite from egg to adult worm. The nematodes go through larval development stages from L1 to L5, where the L3 stage is the infective stage. L3 larvae are covered with a protective sheath, which is exsheathed before the nematode can infect the target organ.<sup>84</sup> Larval exsheathment assays are commonly used methods for the assessment of anthelmintic activity of the infective L3 stage larvae.<sup>85–87</sup> For instance, the exsheathment inhibition activity of tannin rich extract has been observed with multiple nematode species such as *Haemonchus contortus*, *Trichostrongylus colubriformis*, *Teladorsagia circumcincta*, *Cooperia oncophora*, and *Ostertagia ostertagi*.<sup>88</sup>

Another common approach, which targets on the L3 stage is the larval migration inhibition assay.<sup>89,90</sup> There are different experimental approaches in the migration

inhibition assays. For instance, on a 96-well plate format a removable screen plate utilising 20  $\mu\text{m}$  pore size has been observed to let the L3 larvae migrate through, yet it prevents the migrated larvae from falling back.<sup>91,92</sup> Another functional approach is the use of solidified agar solution.<sup>89,93</sup> The migration inhibition assay utilising agar has been successfully used with *Ascaris suum* L3 larvae (Figure 5). In this method, the larvae and agar in water are mixed together. After the agar has solidified, the larvae are let to migrate on top of the agar, where the migrated larvae are counted.<sup>89</sup> Even though, the *A. suum* is not a ruminant nematode, the larval migration inhibition assay with *A. suum* stage L3 larvae functions as a highly reproducible *in vitro* model system for variable nematodes.<sup>94,95</sup>

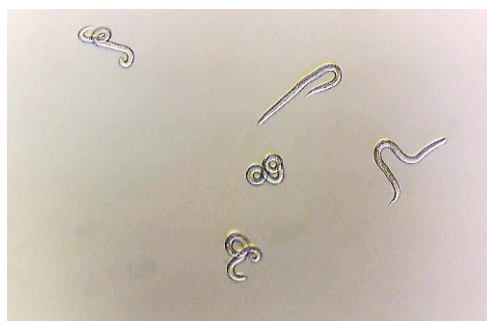


**Figure 5.** Stage L3 larvae of *Ascaris suum* in RPMI-1640 medium as seen by inverse light microscope.

Remarkably, the similar structural features of PAs are linked to the anthelmintic activity as well as protein binding affinity and it has been proposed that the mode of action towards nematodes could take place via protein binding.<sup>87</sup> Multiple studies have shown that the anthelmintic activity of PAs increase with their mDP and it seems to be the key factor for anthelmintic activity.<sup>83,89,90,96,97</sup> The effectiveness of PD units over PC units has been observed as well both in the case of PA rich fractions<sup>98</sup> and monomers<sup>99</sup>. Another PA structural feature increasing anthelmintic activity is the galloylation of the flavan-3-ol units.<sup>95,100</sup> The effect of stereochemistry (*cis/trans* ratio) only had a minor effect on the activity slightly favouring *cis* enantiomers over *trans* enantiomers.<sup>97</sup> Even though these generalisations have been agreed on by several researchers, the effect of the above listed structural features vary greatly in different nematodes, larval development stages and also depending on the plant sources of the studied PAs.<sup>97,98</sup>

### 1.4.3 Bioavailability

In agriculture, PA rich feeds are usually preserved as hay, pellets or silage.<sup>83</sup> Therefore, in addition to the knowledge of direct effects of PAs, the fate of these compounds during preservation must be known as well. The feed treating practises include for example pelleting<sup>101</sup> and ensiling<sup>102</sup> and significant changes in the PA composition have been observed during these processes. In the plant material, the PAs can be in either extractable or non-extractable form.<sup>103,104</sup> The non-extractable PAs can be bonded with protein or fiber.<sup>103,105</sup> Significant changes in the PA composition and concentration have been observed after wilting, ensiling and pelleting of PA rich plant materials suggesting that some part of the extractable PAs are transformed into non-extractable form.<sup>101,106</sup>



**Figure 6.** *Trifolium repens*, a highly prodelphinidin rich plant species.

The preservation of plant material and the changes in the content and concentration of extractable and non-extractable PAs does not necessarily mean weaker bioactivity. For instance, pelleted sericea lespedeza has been successfully used to treat GIN infections in goats.<sup>107</sup> Ramsay et al<sup>108</sup> hypothesised, that the protein or fibre bound PAs could function in the small intestine as anthelmintics after dissociation from the complex.

In addition to the complexation of PAs and protein or fibre during ensiling or other preservative processes, the complexation can take place in the digestive track of ruminants as well. For instance, PAs can form non-covalent PA-protein complexes with dietary proteins in rumen at neutral conditions (pH 6–7) and then decompose in the abomasum at acidic conditions (pH < 3.5) releasing the protein into the digestion.<sup>109,110</sup> This could have implication for the protein digestibility.<sup>111</sup>

The interactions between PAs and macronutrients such as proteins or fibre are without a doubt complex field of study. The complexation can take place during the preservation process<sup>101,105,106</sup> of feeds or in the digestive track of ruminants<sup>109,110</sup>. Different effects on the animal health such as modified protein digestibility<sup>111</sup> or anthelmintic activities<sup>107</sup> have been hypothesised to be caused by nutritional PAs. Still, more studies on this field are needed to better understand these interactions.

## 2 Materials and Methods

### 2.1 Isolation and purification of proanthocyanidins

#### 2.1.1 Extraction

##### Large scale extraction for proanthocyanidin purification

Fresh plant material was collected into acetone (Figure 7) and macerated at 4°C for 9–12 months. The collected plant species and tissues are listed in Table 1. After maceration, the plant material was ground and extracted 4 to 6 times with 4/1 acetone/water (v/v). The extracts were brought to water phase and lyophilised.



**Figure 7.** Freshly collected plant material in acetone. Photo kindly provided by Anne Koivuniemi.

##### Vicia faba samples

The collected *Vicia faba* samples were crimped and ensiled in seven different treatments in three replicates each (see Table 1 in **IV**). Ensiled, dried and grinded *Vicia faba* seed samples (**IV**) were weighed (20.0 mg) and extracted with 1400 µl of 4/1 acetone/water, v/v twice for 3 h. The first extract batch was added one day before

extraction and the samples were macerated at 4 °C overnight. The extracts were combined, brought to water-phase and freeze-dried. Prior UPLC-DAD-QqQ analysis, the samples were diluted with 1000 µl of water, shaken thoroughly and filtered with 0.2 µm PTFE syringe filters.

**Table 1.** The plant sources used in this PhD project. Table adapted from Leppä et al. (I)

Plant species		Sephadex FR 6 compositions		
Latin name	Plant tissue	<sup>a</sup> mDP	<sup>b</sup> PC/PD ratio	<sup>c</sup> EG (mol/mol)
<i>Aesculus hippocastanum</i> L.	leaves	4	99/1	-
<i>Trifolium medium</i> L.	flowers	9	99/1	-
<i>Rhododendron dichroanthum</i> Diels.	leaves	5	79/21	1.0
<i>Rhododendron schlippenbachii</i> Maxim.	leaves	6	78/22	1.3
<i>Larix</i> sp	needles	12	62/38	-
<i>Lotus corniculatus</i> L.	green brownish pods	14	45/55	-
<i>Lysimachia vulgaris</i> L.	flowers	20	27/73	-
<i>Pinus sylvestris</i> L.	needles	18	24/76	-
<i>Salix phylicifolia</i> L.	leaves	20	15/85	-
<i>Ribes alpinum</i> L.	leaves	19	3/97	-
<i>Trifolium repens</i> L.	flowers	18	2/98	-

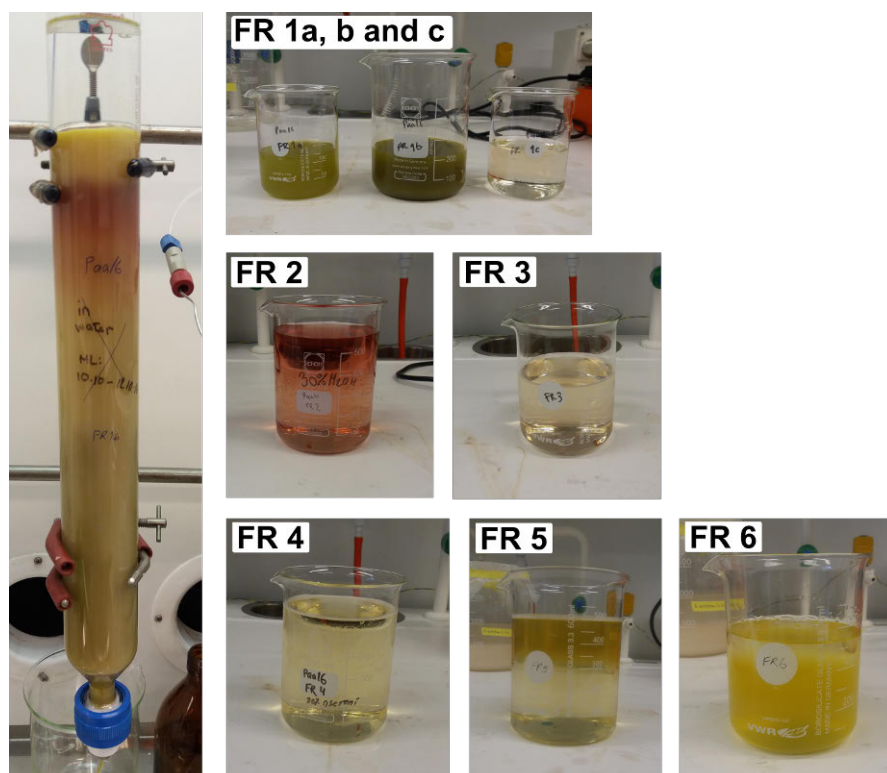
<sup>a</sup>Mean degree of polymerisation (mDP) and <sup>b</sup>ratio of procyanidin and prodelphinidin subunits (PC/PD) measured by UPLC-MS/MS<sup>29</sup>. <sup>c</sup>Estimated galloyl content in relation to proanthocyanidin content.

### 2.1.2 Sephadex LH-20 fractionation

The dried extracts (approx. 8–10 g) were dissolved in water and the insoluble impurities were removed by centrifugation and filtration (0.45 µm PTFE). The fractionation was carried out with Sephadex LH-20 column (40 × 4.0 cm Chromaflex®, Kontes) in step-by-step elution protocol (Table 2). Approximately 500 mL of each Sephadex LH-20 fraction (FR) was collected and based on the colour of the column, some fractions were collected in two or more sub-fractions (Figure 8). The fractions were brought to water-phase *in vacuo* and lyophilised.

**Table 2.** The elution protocol of the Sephadex LH-20 fractionation.

Collected fraction (FR)	Eluent composition
FR 1	water
FR 2	methanol/water 3/7 (v/v)
FR 3	methanol/water 1/1 (v/v)
FR 4	acetone/water 3/7 (v/v)
FR 5	acetone/water 1/1 (v/v)
FR 6	acetone/water 4/1 (v/v)

**Figure 8.** The Sephadex LH-20 fractionation of *Lysimachia vulgaris*.

### 2.1.3 Semipreparative purification

The sixth Sephadex LH-20 fractions (FR 6) were used as source material in the semipreparative purification (Table 1). The detailed description of the semipreparative purification is given in Leppä *et al.* (I). In short, approximately 125 mg of dried FR 6 material was diluted in 3 mL of water. The fractionation was

carried out with an HPLC instrument equipped with a  $150 \times 21.20$  mm, Gemini® 10  $\mu\text{m}$ , C-18, 110A, Axia packed (Phenomenex) column.

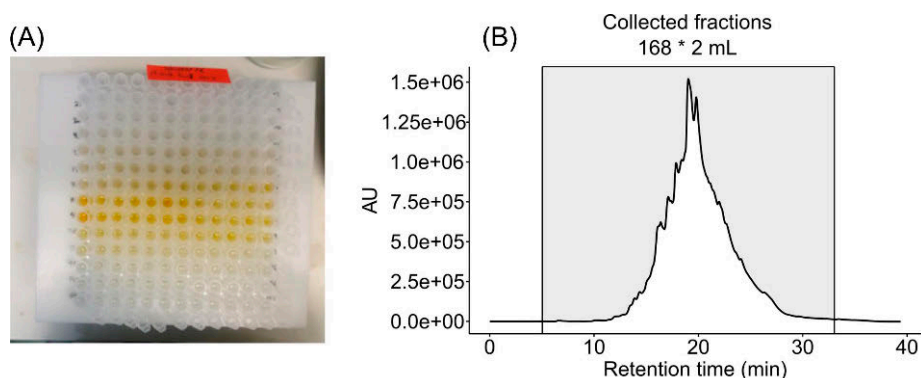


**Figure 9.** Semipreparative fractionation of *Rhododendron dichroanthum* as (A) collected 168 sub-fractions and (B) as seen with DAD trace at 280 nm. Figure B panel adapted from Leppä et al. supplementary material (II).

The elution utilised acetonitrile (A) and 0.1/99.9 formic acid/water (v/v) (B) in gradient elution mode as follows: 0–4 min, isocratic 8% A in B; 4–32 min, 8–55% A in B (linear gradient); 32–35 min, 55–80% A in B (linear gradient), 35–80 min column wash and stabilisation. The flow rate was set to  $12 \text{ mL min}^{-1}$  and fractions (fr) were collected from 5 to 33 min (Figure 9). The elution of the PAs was detected with diode array detector (DAD) at 280 nm and every fourth fraction along the PA fingerprint was analysed with UPLC-DAD-QqQ and UPLC-DAD-Q-Orbitrap. Approximately 25–35 fractions were analysed per each plant species resulting in total of 350 analysed fractions.

## 2.2 Mass spectrometric analysis

### 2.2.1 UPLC-DAD-QqQ

The MS/MS analyses<sup>29,30</sup> were carried out with a Xevo TQ triple quadrupole mass spectrometer (Waters Corp., Milford, MA, USA) coupled with an Acquity UPLC system (Waters Corp., Milford, MA, USA). Samples were analysed with a Waters Acquity UPLC BEH Phenyl column ( $1.7 \mu\text{m}$ ,  $2.1 \times 100$  mm Waters Corp. Wexford, Ireland). Acetonitrile (A) and 0.1/99.9 formic acid/water (v/v) (B) were used as eluents in gradient elution protocol starting with isocratic 0.1% A in B for 0–0.5 min followed by 0.1–30% A in B linear gradient for 0.5–5.0 min and 30–45% A in B linear gradient for 5.0–8.0 min following column wash and stabilization for 8.0–

11.0 min. The flow rate was set to 0.5 mL min<sup>-1</sup> and the UV ( $\lambda = 190\text{--}500$  nm) and MS data was recorded at 0–8 min. Catechin solution (1  $\mu\text{g mL}^{-1}$  in acetonitrile/0.1% formic acid (2/8, v/v)) was used to monitor the stability of the MS/MS response as described by Malisch *et al.*<sup>112</sup>

Similar ion source parameters were used as described earlier (I) and the quantitative analysis of PC, PD and galloyls as well as the determination of mDP were carried out with the Engström method<sup>29,30</sup> as described by Leppä *et al.* (II). In short, the integrated areas of galloyls were quantified against 1,2,3,4,6-penta-*O*-galloylglucose. The PC, PD and mDP were quantified against previously prepared PA rich Sephadex LH-20 fractions with known PC/PD ratio and mDP. The PC standard was isolated from *Tilia* flowers (PC/PD 95/5), PD standard from *Ribes nigrum* leaves (PC/PD 1/99) and the mDP standards from *Vaccinium vitis-idaea* leaves, *Calluna vulgaris* flowers and *Tilia* flowers (mDP 2.2, 3.5, 3.6, 4.1, 6.0 and 9.9). The integrations were carried out with Target Lynx software (V4.1 SCN876 SCN 917 © 2012 Waters Inc.).

In order to visualise the PA fingerprints effectively as a function of retention time ( $t_R$ ), the PA concentration in each time point was calculated with PC and PD calibration curves resulting in concentration-based corrected raw traces (concentration corrected abundance, CCA). Also, the estimated galloyl content in relation to PA content (EG) was calculated based on the quantitative results. The  $t_R$  values of each analysed fraction was obtained from the peak top time.

## 2.2.2 UPLC-DAD-Q-Orbitrap

The HRMS analyses were carried out with quadrupole–Orbitrap instrument (Q Exactive<sup>TM</sup>, Thermo Fisher Scientific GmbH, Bremen, Germany), which was coupled to a similar Aquity UPLC system (Waters Corp., Milford, MA, USA) as was used with the MS/MS analyses. The column used was an Acquity UPLC BEH Phenyl 1.7  $\mu\text{m}$ , 2.1  $\times$  30 mm. Acetonitrile (A) and 0.1/99.9 formic acid/water (v/v) (B) were used as eluents. The elution protocol at flow rate 0.65 mL min<sup>-1</sup> started with 0–0.1 min isocratic phase with 3 % A in B, following by 0.1–3.0 min linear gradient with 3–45 % A in B, and lastly finishing with 3.0–4.2 min column wash and stabilisation. The UV ( $\lambda = 190\text{--}500$  nm) and mass ( $m/z = 200\text{--}3000$ , resolution = 70 000, automatic gain control =  $3 \times 10^6$ ) data were recorded throughout the analysis and the analytes were detected as negative ions. The ion source parameters were as described in Leppä *et al.* (I). Thermo Xcalibur (version 4.1) software was used in the analysis of data. The interpretation of the mass spectra was carried out with Qual Browser and the extracted ion chromatograms (EIC) were generated via Quan Browser at  $m/z$  range of 577.11–577.16 for dimeric PC dimers.

## 2.3 Turbidimetric assay

The same every fourth fraction, which were analysed by UPLC-QqQ and UPLC-Q-Orbitrap were measured for their protein precipitation capacity (PPC) via well-plate reader assay (II). Exactly 1400  $\mu\text{l}$  of each fraction was lyophilised prior turbidimetric analysis. The samples were analysed in 5 to 0.4-fold concentration in comparison to the original fractions. The samples were diluted in water prior analysis. The absorbance at  $\lambda = 414 \text{ nm}$  was measured via Multiskan Ascent (354, Thermo Electron Corporation) as follows. Equal volumes (75  $\mu\text{l}$  + 75  $\mu\text{l}$ ) of sample or reference sample solution and bovine serum albumin (BSA) solution in pH 5 buffer (0.05 M acetate supplemented with 60  $\mu\text{M}$  ascorbic acid) were added into the wells and mixed with the well-plate reader. The absorbance was read 31 times in 1 min intervals and the plate was shaken before every reading. Samples were measured in duplicates and the absorbance of the reference sample was deducted from the average absorbance of the samples. The PA concentrations of the samples measured with UPLC-MS/MS were taken into account in the calculations of results (II).

## 2.4 *Ascaris suum* in vitro assay

### 2.4.1 Proanthocyanidin samples

The PA rich sample material for the *in vitro* studies was prepared by combining the semipreparative fractions, which were produced as previously described in this thesis (2.1 Isolation and purification of proanthocyanidins). To obtain enough sample material, 168 fractions of the collected PA fingerprint were pooled in 10 equal sub-fractions based on their UV area at 280 nm, thus resulting in 111 fractions in total (11 plant species  $\times$  10 sub-fractions per plant = 111 pooled fractions).

### 2.4.2 Nematodes

The utilised stage L3 nematodes of *Ascaris suum* were hatched from the previously collected embryonated *Ascaris suum* eggs.<sup>113</sup> The eggs were decoated upon collection with NaOH and stored at +4 °C in 1 M H<sub>2</sub>SO<sub>4</sub>.<sup>89</sup> The eggs were washed 3–4 times with Hank's Balanced Salt Solution (HBSS) and they were hatched by grinding them gently with glass beads in HBSS at +37 °C, 5 % CO<sub>2</sub> in air for 40–60 min. The larvae were separated from the debris overnight via Baerman funnel in sterile HBSS at +37 °C, 5 % CO<sub>2</sub> in air.

### 2.4.3 Migration inhibition and mortality assay

The larval suspension was prepared from cell culture media (RPMI 1640 medium supplemented with 2 mM L-glutamine, 100 U/mL penicillin, and 100  $\mu\text{g mL}^{-1}$  streptomycin) and collected larvae. The larval concentration was set to 0.67  $\text{mL}^{-1}$  and 145  $\mu\text{L}$  of larval suspension was dispensed into a 96-well cell culture plate. The tannin samples (3.0  $\text{mmol L}^{-1}$  in DMSO/water for injection (WFI), 1/1, (v/v)) were added into the plates by mixing 5  $\mu\text{L}$  of tannin solution into the larval suspension. Sample solvent (DMSO/WFI, 1/1, (v/v)) was used as negative control and 50  $\mu\text{g/mL}$  ivermectin as positive control. PA and control samples were analysed in 8 replicates. The plates were kept at room temperature for the maximum of 15 min at a time to ensure the viability of the larvae. The PA and larvae were incubated overnight at +37 °C, 5 %  $\text{CO}_2$  in air.

The larval count per each well was calculated under an inverted light microscope. The dead and living larvae were counted separately. After counting, 150  $\mu\text{L}$  of 1.6% agar solution in water (45 °C) was added to each well by evenly mixing the agar into the larval suspension. Half of the agar–larvae mix was moved into a fresh cell culture plate and the agar was let to solidify for 10 minutes. Lastly, 100  $\mu\text{L}$  of RPMI medium was added on top of the wells. The larvae were let to migrate overnight at +37 °C, 5 %  $\text{CO}_2$  in air. The migrated larvae were counted on top of the agar with a direct light microscope. The larval counts of both plates were combined before results calculation. The migration inhibition activity (MIA-%) and larval mortality (LM-%) were calculated relative to the minimal and maximal migration obtained from the control samples.

## 2.5 Statistical methods

The statistical analyses were carried out with R(3.6.1)<sup>114</sup> in RStudio (version 1.2.5019)<sup>115</sup> and the related graphics were produced *via* ‘*ggplot2*’ package<sup>116</sup>. The PPC results were analysed via Partial Least Squares Regression (PLSR) models with ‘*plsdepot*’<sup>117</sup> package in R. The details of the PLSR models are described in further detail in Leppä *et al.* (II).

## 3 Results and discussion

### 3.1 Semipreparative purification of proanthocyanidins

The width of the retention time ( $t_R$ ) windows of the collected semipreparative fractions differed significantly from that of the original PA fingerprints as compared with UPLC-DAD chromatograms at 280 nm (Figure 10). The width of the  $t_R$  windows of the original PA material ranged between 2.0 and 4.5 min, whereas the  $t_R$  windows of the semipreparative fractions ranged from 0.3 to 1.2 min (I). Figure 10 shows, how efficiently the fractionation of *L. vulgaris* divided the original PA fingerprint into tens of individual PA fractions.

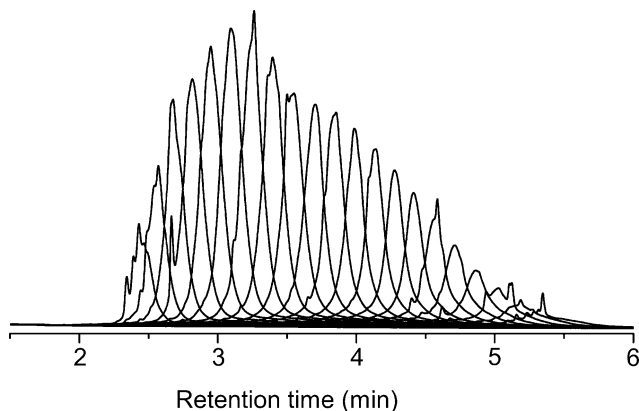


**Figure 10.** The UPLC-DAD ( $\lambda = 280$  nm) chromatograms of every fourth semipreparative fraction of *Lysimachia vulgaris* between fraction number 35 and 115. Figure adapted from Leppä *et al.* (I).

## 3.2 Proanthocyanidin composition of semipreparative fractions

### 3.2.1 UPLC-DAD-QqQ

The MS/MS data revealed the structural features of PAs present in the semipreparative HPLC fractions, such as the proportion of PC and PD units as well as the mDP. Figure 4 (in **I**) shows the great divergence of different PA fingerprints obtained from eleven plant species. The isolated PA fractions ranged from nearly PC pure (See Figure 4, A–D in **I**) to nearly PD pure (Figure 4, S and T, in **I**). They were also different in molecular size (mDP 4–30) and retention time ( $t_R$  2–6 min). Even the most PC rich fractions (Figure 4, A–D, in **I**) had some variation in the mDP (4–17) and retention time (3.5–6.0 min). For instance, *T. medium* fr 82 (See Figure 4B, in **I**) and *A. hippocastanum* fr 116 (Figure 4C, in **I**) were similar in PC/PD and mDP, yet their  $t_R$  were 4.2 min and 5.5 min, respectively. One possible explanation for this could be, that *A. hippocastanum* contained also A-type PAs, which elute at later retention times than the B-type PAs.

Another interesting aspect about the isolated semipreparative PA fractions was their variability even within a single plant species. A comparison of *L. vulgaris* (Figure 11B) fractions 43 (PC/PD 11/89, mDP 19), 67 (PC/PD 36/64, mDP 23), and 91 (PC/PD 68/32, mDP 27) showed that the PC/PD and mDP changed significantly at different retention times. The Sephadex FR 6 of *L. vulgaris* had a PC/PD of 27/73 and mDP was 20 (Table 1). This means that, even PC rich fractions were isolated from originally PD-rich PA material. The PA composition of the semipreparative fractions varied significantly compared to the composition of the Sephadex LH-20 material. This observation accentuates the vast complexity of the PAs produced by a single plant species. In the following chapter, the more detailed molecular composition of these fractions obtained with HRMS is described.

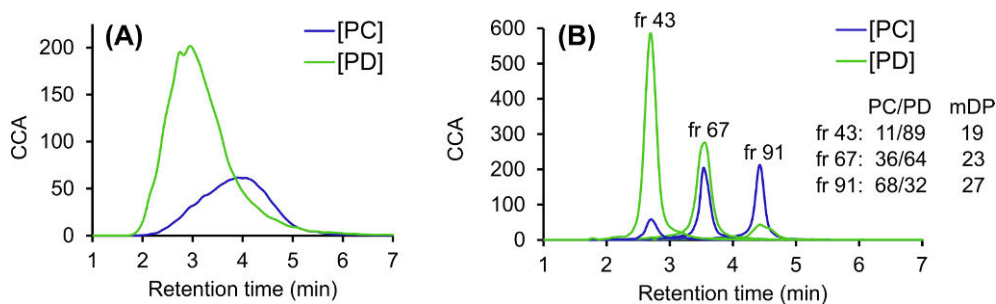


**Figure 11.** A comparison of proanthocyanidin fingerprints of *Lysimachia vulgaris* (A) sixth Sephadex LH-20 fraction and (B) semipreparative fractions (fr) 43, 67 and 91. The figures were produced from UPLC-QqQ traces of procyanidin (PC, blue) and prodelphinidin units (PD, green) and the fingerprints are displayed as concentration corrected abundance (CCA).

The quantitative analysis of the structural features (PC/PD, mDP) enabled the monitoring of the elution of different polymer sizes and PC/PD ratio over retention time. Four different type of plant species (Figure 12) were herein selected to illustrate the changes in the mDP and PC/PD over retention time. The mDP increased in *T. medium* (Figure 12A), *L. vulgaris* (Figure 12C), and *R. alpinum* (Figure 12D), but not in *Larix* sp., (Figure 12B) during the elution. The increase was relatively steady in PC rich *T. medium* (Figure 12A) and PC/PD mixture *L. vulgaris* (Figure 12C). In *Larix* sp. (Figure 12B), the mDP was lowest at the PA concentration maximum. This means, that the majority of the PA composition of *Larix* sp. consisted of relatively small oligomers. The mDP had a local maximum in those plant species, which had relatively homogenous PC/PD, *T. medium* (Figure 12A) and *R. alpinum* (Figure 12D). In these plant species, the largest PAs eluted at the descending part of the PA fingerprint.

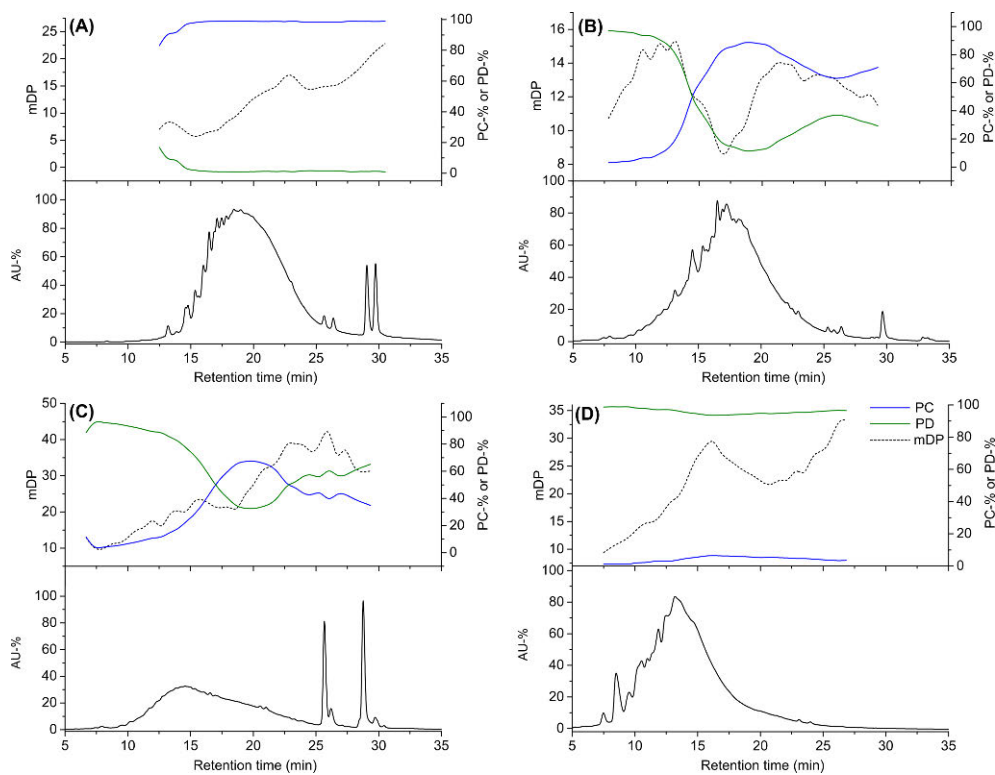


**Figure 12.** Comparison of the semipreparative HPLC DAD traces ( $\lambda = 280$  nm) and the structural features of proanthocyanidins such as the proportion of procyanidin (PC-%) and prodelphinidin (PD-%) units and the mean degree of polymerisation (mDP). The selected plant species for the comparison were (A) *Trifolium medium*, (B) *Larix* sp., (C) *Lysimachia vulgaris*, and (D) *Ribes alpinum*. Figure from Leppä *et al.* (1).

The distribution of PD-% in *Larix* sp (Figure 12B) and *L. vulgaris* (Figure 12C) showed how the most PD rich PAs elute at the beginning of the elution and the PC rich ones at the end of the elution. The PD-% did not decrease steadily in these plant species, yet it increased again at late retention time. The reasoning behind this phenomenon is hypothesised below. Because PD units are considered more hydrophilic than PC units, the elution order should favour PD-rich PAs over PC rich ones in the RP system. This data however indicated that the PD content could increase during the elution. It is also known, that the larger PAs tend to elute later in the RP conditions. Our data also verified that the mDP increased during the elution. In addition, it is also known, that the high mDP is usually associated with high PD-%.<sup>83</sup> Hence, it would seem, that during the elution, the competing forces of increased hydrophilicity due to the higher number of -OH groups and lowered hydrophilicity due to large molecular size find the balance during the elution and thus, the PD-% did not decrease linearly or mDP did not increase linearly either.

### 3.2.2 UPLC-DAD-Q-Orbitrap

The more detailed interpretation of the high-resolution mass spectra can be found in Leppä *et al.* (I). Large proanthocyanidins tend to form multiply charged ions in the ESI source thus enabling the detection of high DP polymers.<sup>37</sup> Depending on the DP, the PAs formed doubly (DP 4–11, Figure 13), triply (DP 10–20, Figure 13) and even four-fold charged ions (DP > 18, Figure 8C in I). Due to the multiply charged ions, certain patterns were observed in the mass spectra (Figure 13). In the case of PC pure samples, the PC pure oligomers and polymers were observed as at  $m/z$   $577.13 + 288.06 \times n$  for singly<sup>42,43</sup>, at  $m/z$   $576.13 + 144.03 \times n$  for doubly and at  $m/z$   $959.87 + 96.02 \times n$  for triply charged ions (Figure 13). In the case of PD pure samples, the PA oligomers and polymers were observed at  $m/z$   $609.12 + 304.06 \times n$  for singly, at  $m/z$   $608.12 + 152.03 \times n$  for doubly and at  $m/z$   $1013.19 + 101.35 \times n$  for triply charged ions, respectively. The symbol  $n$  ( $\geq 0$ ) indicates the addition of one PC or PD unit, respectively. Systematic oligomeric series were observed within each polymer size as well. Within a single oligomer size, the increments of  $m/z$  16.00 for singly, 8.00 for doubly, 5.33 for triply and 4.00 for four-fold charged ions were observed. The increase in  $m/z$  was caused by the increase of the hydroxylation degree of the PA structural units. In conclusion, the different polymerisation and hydroxylation degrees of PAs give rise to these characteristic series of signals, which can be further used in the interpretation of the high-resolution mass spectra of these compounds.

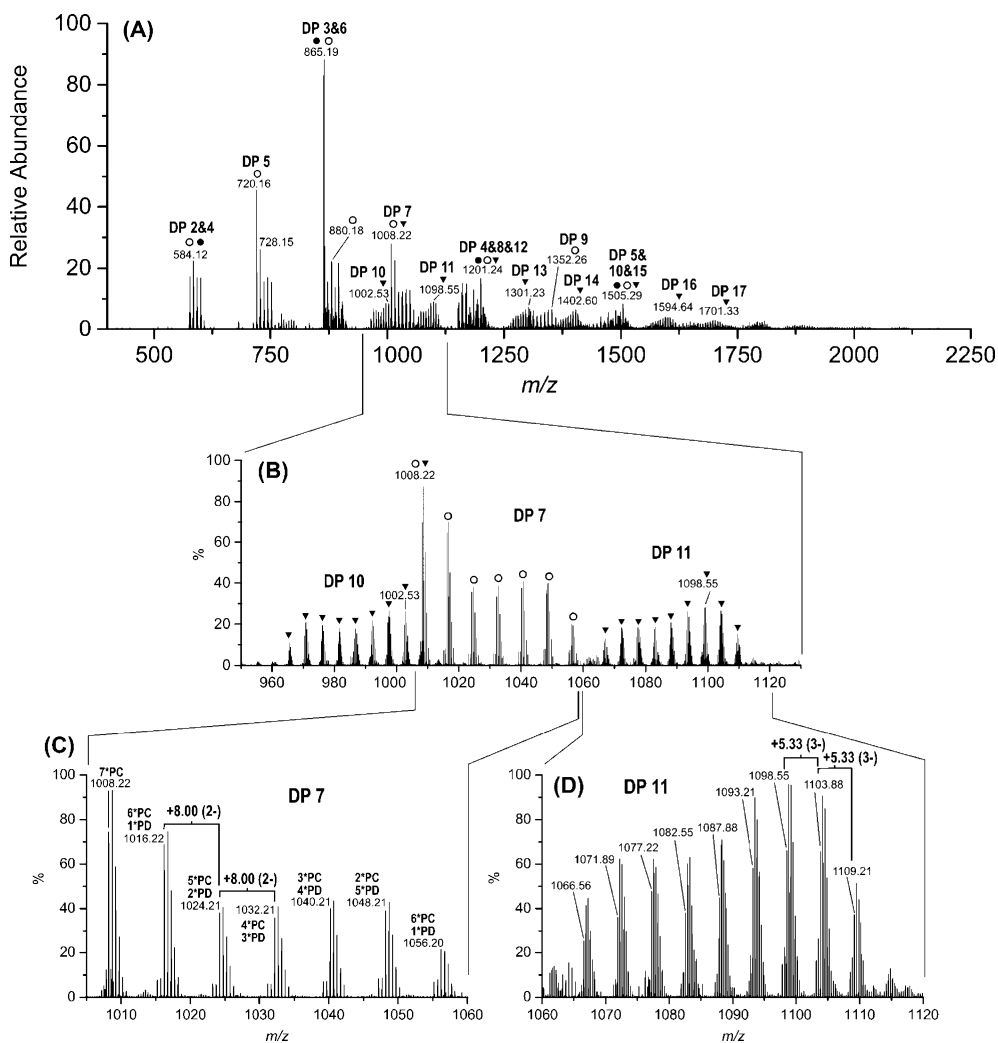


**Figure 13.** High-resolution mass spectra of *Lysimachia vulgaris* semipreparative fraction 67 at  $m/z$  (A) 400–2250, (B) 950–1125, (C) 1005–1060, and (D) 1060–1120. The symbols indicate the charge state of the ions as follows, (●) black dot  $[M-H]^-$ , (○) white dot  $[M-2H]^{2-}$ , (▼) inverted triangle  $[M-3H]^{3-}$ . DP refers to degree of polymerisation. See Table 2 (in I) for interpretations. Figure from Leppä *et al.* (I).

Differences between semipreparative fraction 67 (Figure 13) and 91 (see Figure 8 in I) of *L. vulgaris* demonstrated the changes in PA composition in fractions, which were collected at different retention times. The semipreparative fraction 67 (Figure 13, See Table 2 in I) included a mixture of oligomers ranging from PC pure to PD pure and the degree of polymerisation ranged between 4–17 subunits. The semipreparative fraction 91 (Figure 8 and Table 3 in I) consisted mainly from PC-rich oligomers and the polymerisation of the compounds ranged between 5–25

subunits. Larger polymers were identified in the fraction 91 (mDP = 27) than in the fraction 67 (mDP = 23). These findings were in good accordance with the quantitative results from UPLC-MS/MS.

In some plant species in some of the latest eluting semipreparative fractions, the oligomeric series of PAs were observed as what were herein proposed to be HRF fragments. In *Ribes alpinum* semipreparative fr 92, a doubly charged series of oligomeric PAs (DP 4–10) was observed as a series of  $[M-2H-126.03]^{2-}$  ions (Figure 14, Table 3). The neutral loss of 126.03 Da corresponds to the HRF fragment, which is equivalent to the cleavage of A ring from the upmost extension unit.<sup>118</sup> To my knowledge, this is the first time this type of series of fragmented oligomers has been observed.

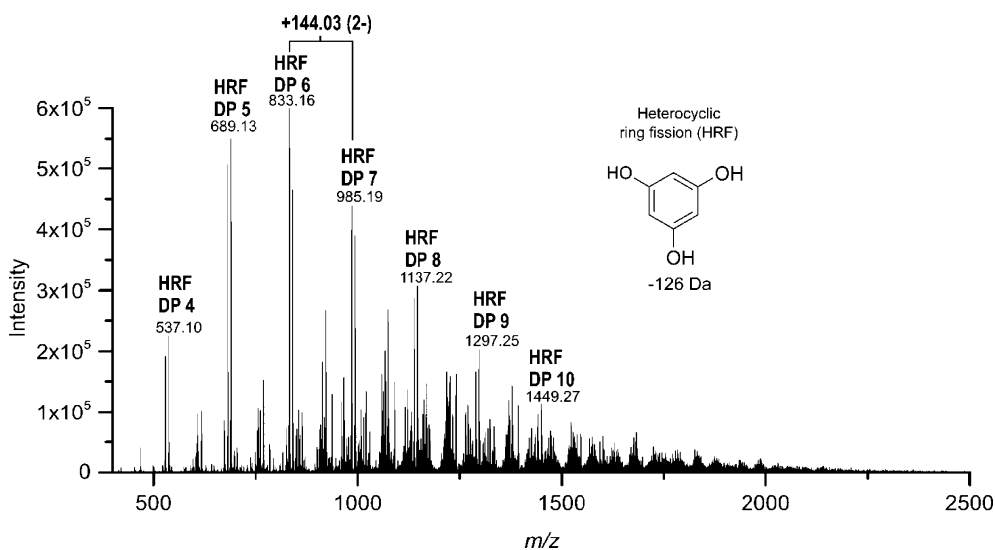


**Figure 14.** High-resolution mass spectra of *Ribes alpinum* semipreparative fraction 92. The doubly charged ions  $[M-2H-126.03]^{2-}$  of heterocyclic ring fission (HRF) fragments of oligomeric series of proanthocyanidin are marked in the spectrum. See Table 3 for interpretations.

**Table 3.** Interpretations of the high-resolution mass spectrum of *Ribes alpinum* semipreparative fraction 92. The numbering of the oligomeric series refers to Figure 14. All interpreted signals were doubly charged heterocyclic ring fission (HRF) fragment ions  $[M-2H-126.03]^{2-}$ .

Oligomer	<i>m/z</i> value of the most abundant $[M-2H-126.03]^{2-}$ ion	Measured accurate mass (amu)	Mass error (ppm)	Number of PC/PD units in the most abundant oligomer	
				PC	PD
DP 4	537.10347	1202.25395	-0.67	1	3
DP 5	689.13251	1506.31226	-0.69	1	4
DP 6	833.16455	1794.37565	-0.19	2	4
DP 7	985.19336	2098.43396	-0.49	2	5
DP 8	1137.22058	2402.49226	-2.04	2	6
DP 9	1297.24547	2722.54548	-3.06	1	8
DP 10	1449.27312	3026.60379	-3.75	1	9

Abbreviations used: amu, atomic mass unit; DP, degree of polymerisation; PC, procyanidin; PD, prodelphinidin; ppm, parts per million.

### 3.3 Protein precipitation capacity of proanthocyanidins

#### 3.3.1 Effect of structural features and retention time

The bioactivity of the previously purified PA fractions was studied via a turbidimetry based well-plate reader method (II). The PPC is shown as a function of the mDP, PD-% and  $t_R$  in Figure 15. The plant species are differentiated by different colours. The PPC increased linearly as a function of the mDP, whereas similar systematic patterns were not observed in the case of PD-% or  $t_R$ . The linear correlation between PPC and mDP in the complete data set ( $r = 0.79$ , II) was strong and ascending. In all plant species, the correlation between PPC and mDP was linear and ascending, yet their correlation coefficients differed slightly ( $r = 0.68$ – $0.93$ , except for *P. sylvestris*  $r = 0.27$ ). For more detailed examination, the separate figures of each plant species are illustrated in Supplementary material of Leppä *et al* (II). The linear increase of activity as a function of the molecular size is in good accordance with the previous literature.<sup>56,57,68,69</sup> The larger molecular size of PAs increases the probability of cross-linkages<sup>56</sup> between soluble PA–protein complexes thus resulting in formation of insoluble complexes.<sup>119</sup>

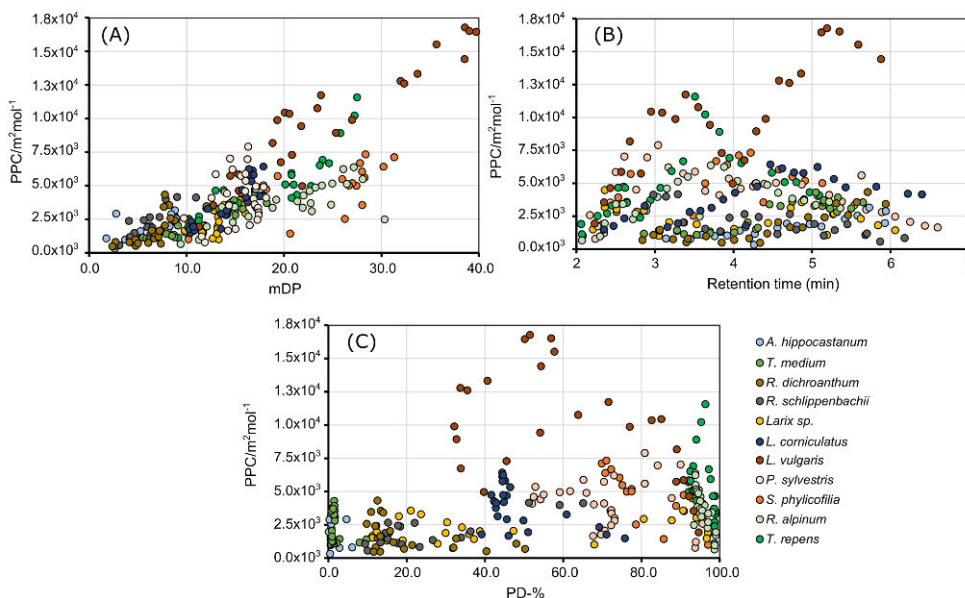


**Figure 15.** The correlation of protein precipitation capacity (PPC) as a function of the (A) mean degree of polymerisation (mDP), (B) retention time of fractions and (C) proportion of prodelphinidin (PD-%) of all studied plant species. Individual plant species are presented with different colours. The correlation of the complete data set was  $r = 0.79$ . Figure from Leppä *et al.* (II).

The correlation between PD-% and PPC were slightly negative in the majority of the samples. This was especially shown in the most PD rich plant species such as *L. vulgaris* (Figure S3,G in II), *S. phlycifolia* (Figure S3, I in II), *R. alpinum* (Figure S3,J in II) and *T. repens* (Figure S3,K in II). This is an interesting observation, as in theory the greater amount of hydroxyl groups should increase the probability of hydrogen bonding between PA and BSA and thus ought to increase the complex formation and eventually the precipitation of complexes.<sup>119</sup> In this particular case, the high PD-% fractions were also low in mDP as compared to the other fractions isolated from the same plant. Therefore, they had lower activity due to smaller oligomer size than the fractions with lower PD-% and higher mDP.

The distribution of PPC within the 2–7 min  $t_R$  window was different in plant species, which were different in their PA composition. In order to compare the distribution of PPC and PA composition, the PPC curves as a function of  $t_R$  were plotted over PA fingerprints (Figure 16).<sup>29,120</sup> For instance, in PC rich plant species such as *A. hippocastanum* (Figure 16,A), *T. medium* (Figure 16,B) and *R. dichroanthum* (Figure 16,C) the activity increased at late  $t_R$ . This means that the most PPC active compounds eluted mainly at the descending part of the PA fingerprint and the most active compounds were in minor concentrations.

Especially in PD containing plant species, the PPC followed a second order polynomial curve as a function of  $t_R$  (Figure 16). This was systematically observed with the most PD rich plants such *R. alpinum* (Figure 16,J) and *T. repens* (Figure 16,K). In these plant species, the compounds with the highest PPC eluted approximately 0.5 min after the concentration maximum thus indicating that the most abundant compounds were not the ones with the highest PPC.

The distribution of PPC over 2–7 min  $t_R$  area was rather irregular in those plant species, which contained more homogenous PC/PD ratio. For instance, *Larix* (Figure 16,E), *L. vulgaris* (Figure 16,G) and *P. sylvestris* (Figure 16,H) contained two PPC maxima as a function of the  $t_R$ , whereas the PPC in *L. corniculatus* (Figure 16,F) followed a second order polynomial curve as in the case of PD rich plant species. Unlike in the majority of the plant species, in *P. sylvestris* the PA concentration maxima overlapped the PPC maxima suggesting that the most concentrated PA fractions were also high in PPC. In *S. phlycifolia* (Figure 16,I) the distribution of PPC was rather irregular. Both ascending and descending parts of the PA fingerprint had relatively high PPC, but the concentration maximum had relatively low PPC.



Unexpectedly, both galloylated plant species *R. dichroanthum* (Figure 16,C) and *R. schlippenbachii* (Figure 16,D) had a completely different distribution of PPC over  $t_R$  despite their similar PC/PD and mDP. As earlier described, in *R. dichroanthum* the PPC increased while the  $t_R$  increased. *R. schlippenbachii* was the only plant species, where the PPC systematically decreased at later  $t_R$ .

In conclusion, the maximal PPC cannot be necessarily estimated based on the PA fingerprint of the plants. In either extremely PC or PD rich plant species, the distribution of PPC was rather consistent, but in more heterogeneous PC/PD mixtures, the distribution patterns were merely irregular. Only in few plant species, the most concentrated PA fractions contained the highest PPC. In majority of the plants, the PPC maxima were either at the ascending, descending or both parts of the PA fingerprint. This means, that knowing the complete activity of the plant PAs is crucial. For example, by examining only the most concentrated fractions, the complete PPC of the plant species could be significantly underestimated.

The statistical analysis of the turbidimetry results showed similar observations as was obtained via UPLC-MS/MS results (II). The results were analysed via Partial Least Square Regression (PLSR, Figure 17) and the same variables were included in the models as was studied above (mDP, PD-%,  $t_R$  and EG). The  $t_R$  was also included as quadratic variable ( $t_R^2$ ) in those plant species, where the distribution of PPC followed a second order polynomial curve as a function of  $t_R$  (Figure 16). Retention time ( $t_R$  and  $t_R^2$ ) and structural features of PAs (mDP and PD-%) explained 64.2 % of the measured variation of the PPC in the complete data set and the model was not over-fitted to this specific data set ( $Q^2 = 0.614$ ). The most significant variable for the PPC was mDP (regression coefficient 0.799) whilst the other variables were not significant. The relevance of mDP to the PPC was in good accordance with the UPLC-MS/MS results and previous literature.<sup>56,57,68,69</sup> The plant species specific PLSR models explained 49.9–89.2 % of the measured variance of PPC and these models were not over-fitted either ( $Q^2 = 0.378–0.858$ ). More detailed examination of the relevant values such as regression coefficients, the coefficients of determination ( $R^2X$  and  $R^2Y$ ) and cross-validated  $R^2$  values ( $Q^2$ ) are presented in Leppä *et al.* (Table 1, in II).

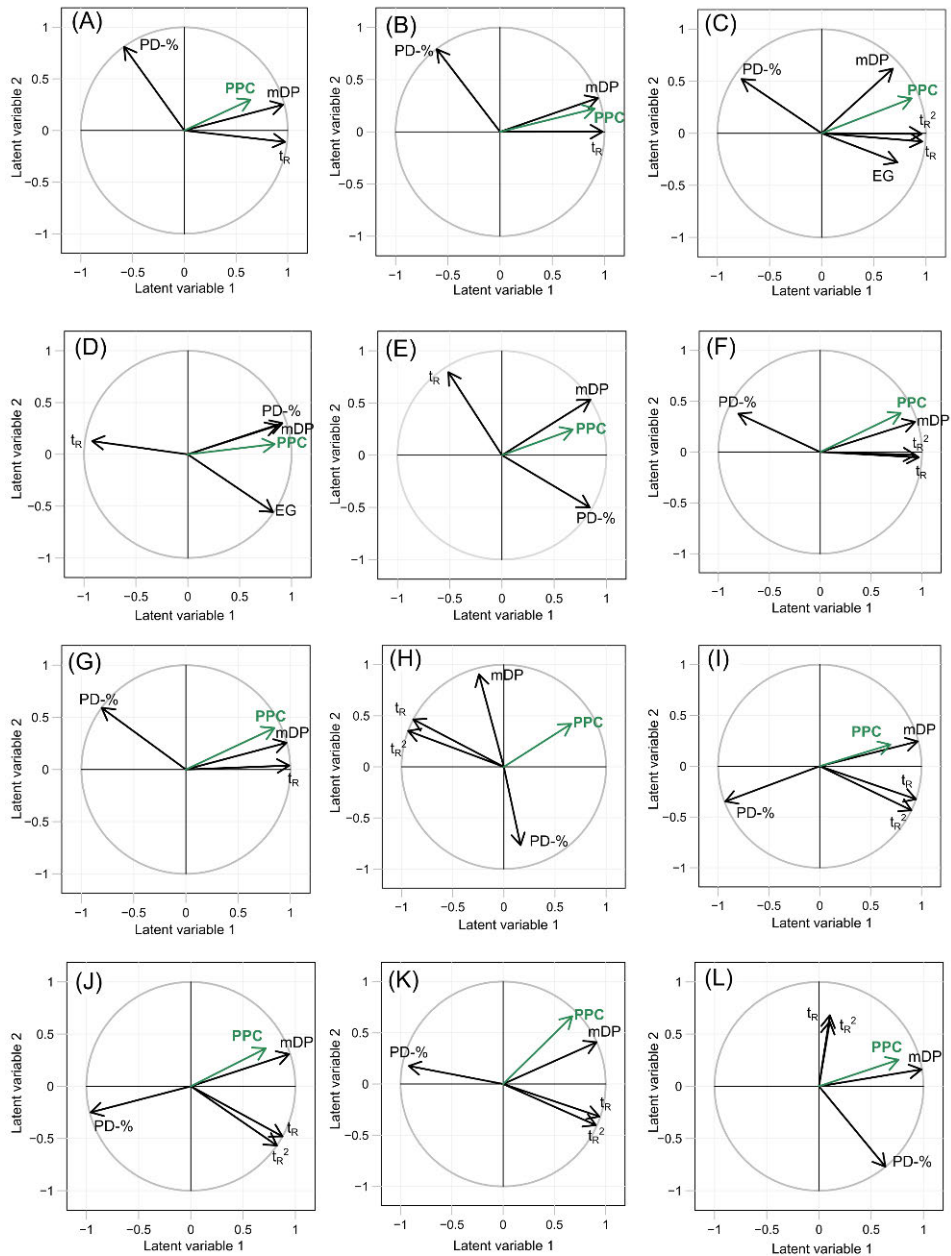


**Figure 17.** The Partial Least Squares Regression correlation circles of (A) *Aesculus hippocastanum*, (B) *Trifolium medium*, (C) *Rhododendron dichroanthum*, (D) *Rhododendron schlippenbachii*, (E) *Larix* sp., (F) *Lotus corniculatus*, (G) *Lysimachia vulgaris*, (H) *Pinus sylvestris*, (I) *Salix phylicifolia*, (J) *Ribes alpinum*, (K) *Trifolium repens* and (L) all the plant species. The abbreviations are as follows; protein precipitation capacity (PPC), quadratic term of retention time ( $t_R^2$ ), retention time ( $t_R$ ), mean degree of polymerisation (mDP), prodelphinidin proportion (PD-%) and the estimation of the relative galloyl content (EG). Figure from Leppä et al. (II).

Another key observation from the PLSR models, which supported the UPLC-MS/MS results was the similarities in regression coefficients in extremely PC or PD rich plant species. This means, that the PPC was caused by the same factors in those plant species, which contained similar PA compositions. For instance, in PD rich plant species *R. alpinum* (PC/PD = 3/97) and *T. repens* (PC/PD = 2/98) the similar correlation coefficients (see Table 1 in II) and the vector plots (Figure 17, J and K, respectively) showed that the PPC was caused by the same features out of which, mDP was the main factor increasing the PPC. On the other hand, in PC rich plant species *A. hippocastanum* (PC/PD = 99/1) and *T. medium* (PC/PD = 99/1) (Figure 17, A and B) the increase in both mDP and  $t_R$  increased the PPC significantly.

The PLSR results also showed that the factors causing the PPC in galloylated and relatively homogenous PAs, were inconsistent as was already observed from the irregular distribution of PPC over  $t_R$  in these kind of plant species. Nevertheless, in all of these plant species, the increase in mDP increased PPC. In plant species with variable PC/PD (*Larix sp.*, *L. corniculatus*, *L. vulgaris*, *P. sylvestris* and *S. phylicifolia*, (Figure 17,E–I, Table 1 in II), the strength of the correlation between mDP and PPC varied greatly. Especially, in those plant species where the correlation was strong (*L. corniculatus* and *L. vulgaris*, regression coefficients 0.926 and 0.754, respectively) also the PLSR models explained the variation of the PPC better (*L. corniculatus*,  $R^2 = 0.773$  and *L. vulgaris*,  $R^2 = 0.875$ ) than in those plant species, where the correlation was weaker (*Larix sp.*, *P. sylvestris* and *S. phylicifolia*, regression coefficients 0.650, 0.607 and 0.379 and  $R^2 = 0.521$ , 0.611 and 0.526, respectively). This finding could indicate that there are probably other structural features in *Larix sp.*, *P. sylvestris* and *S. phylicifolia* besides mDP and other factors measured in this study, which credited more to the PPC.

### 3.3.2 Fraction by fraction comparison of *Ribes alpinum*

The comparison of individual fractions of *R. alpinum* showed how the PPC decreased at  $t_R = 3.4\text{--}3.8$  min (fraction numbers 64, 68 and 72, Figure 18). The high-resolution mass spectra of these fractions revealed that the low PPC fraction 68 contained dimeric PC, which was not observed in notable traces in fractions 64 and 72. The extracted ion chromatogram (EIC) of dimeric PC (at  $m/z = 577.11\text{--}577.16$ ) showed that the decrease in PPC was completely opposite to the increase in the abundance of dimeric PC in the fractions (Figure 18). This observation could indicate that the drastic decrease in PPC in these mainly PD rich, high mDP fractions was caused due to the coelution of considerably smaller PC pure oligomer. This finding emphasises the importance of understanding how differences in PA composition can affect their total activity.

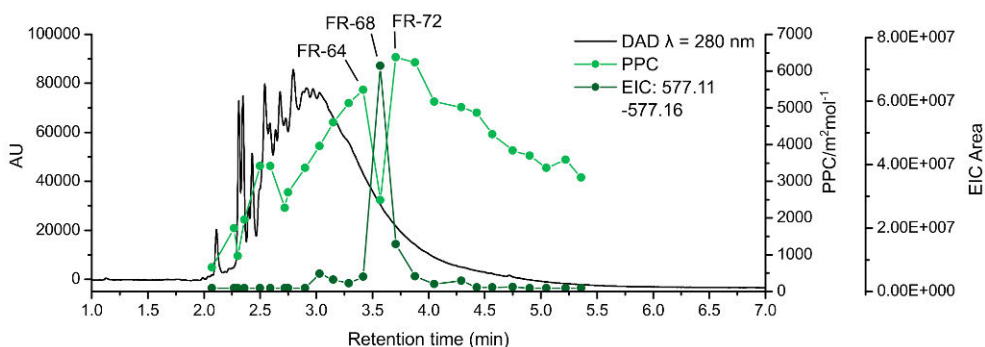


**Figure 18.** UPLC-DAD chromatogram ( $\lambda = 280$  nm) of *Ribes alpinum* (black line). The protein precipitation capacity (PPC, light green dots and line) and the peak areas of extracted ion chromatograms of the dimeric B-type procyanidin (EIC at  $m/z$  577.11–577.16, dark green dots and line) are presented on top of the chromatogram. Figure from Leppä et al. (II).

## 3.4 Anthelmintic activity of proanthocyanidins

### 3.4.1 Effect of structural features and retention time

The anthelmintic activity of the purified PAs was studied via migration inhibition activity (IA-%) and larval mortality (LM-%) assays against *Ascaris suum* stage L3 larvae (III). Both anthelmintic assays showed an increase in activity as the mDP increased (Figure 19). The IA-% followed a logarithmic curve as a function of the mDP ( $y = -23.3 + 36.6 \times \ln(x)$ ,  $R^2 = 0.67$ , Figure 19A), whereas the increase in LM-% was linear ( $y = 4.41 + 0.601 \times x$ ,  $R^2 = 0.28$ , Figure 19B). The results from LM-% (< 44%) showed in general lower activity values than IA-% (=0–100%), which is natural since, the migratory inhibitory activity is a sub-lethal activity measure and will emerge at lower PA concentration.

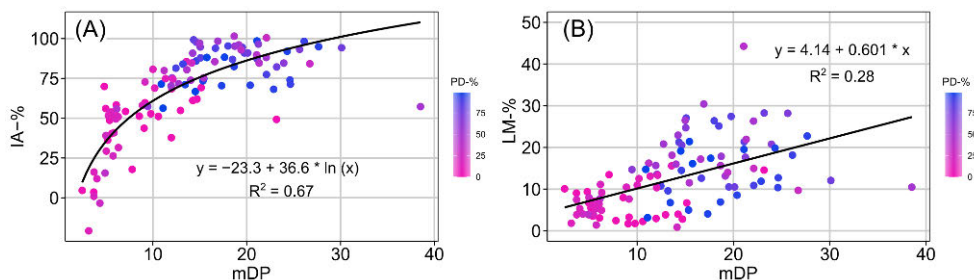


**Figure 19.** (A) Migration inhibition activity (IA-%) and (B) larval mortality (LM-%) of the studied proanthocyanidin samples as a function of mean degree of polymerisation (mDP). The proportion of prodelphinidins (PD-%) is illustrated as colour gradient (blue: PD-% = 100%, pink: PD-% = 0 %). Figure from Leppä et al (III).

The PD-% was illustrated with a colour gradient in order to show the distribution of PC/PD composition over the activity range and different polymer sizes (Figure 19). In general, both activity measures showed that the mDP and activity increased as the PD-% increased. In other words, the fractions with low mDP and PD-% were the least active ones, whereas the high mDP and PD-% fractions were the most active ones. Figure 19A showed that the majority of the significantly inhibitive fractions (IA-% > 75 %) were high in PD-%. Also, the majority of the low mDP (< 10) fractions were solely PC rich.

Figure 20 shows the distribution of IA-% and LM-% over the retention time area of the isolated fractions. As previously, the colour gradient was used to illustrate the PC/PD composition of the fractions and the size of the data points represent the mDP. The most inhibitory active fractions (IA-% > 90 %, Figure 20A) did not elute at a certain  $t_R$  area, since their  $t_R$  range covered  $t_R = 2.8$ – $5.3$  min. On the other hand, it

seemed that the fractions with the lowest activity eluted relatively late at  $t_R = 3.3$ – $5.5$  min (Figure 20B). Since the LM-% values were lower than the ones of IA-%, the differences in activity were less distinctive. Nevertheless, the majority of the high LM-% (>20%) fractions eluted relatively early ( $t_R < 4.0$  min). Figure 20 also intuitively shows how the elution of PC and PD rich fractions differed from one another. Generally speaking, the majority of PD rich fractions eluted at  $t_R = 2.0$ – $4.0$  min, whereas PC rich fractions eluted at  $t_R = 3.3$ – $5.5$  min. This observation is in good accordance with the earlier literature.<sup>121</sup>

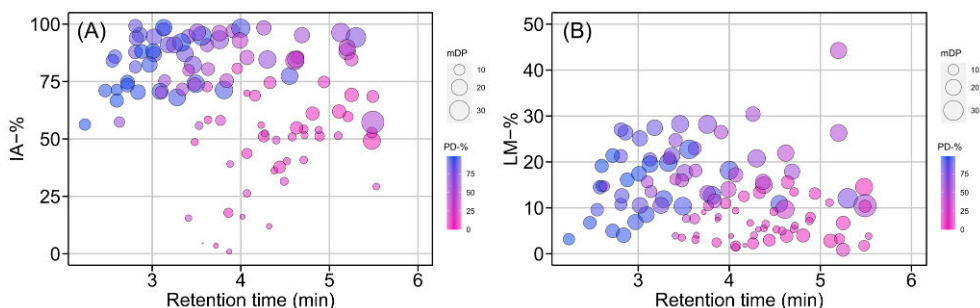


**Figure 20.** Migration inhibition activity (IA-%) and (B) larval mortality (LM-%) of the studied proanthocyanidin samples as a function of the retention time of the fractions. The proportion of prodelphinidins (PD-%) is illustrated with colour gradient (blue: PD-% = 100-%, pink: PD-% = 0 %). The size of the bubbles illustrated the mean degree of polymerisation (mDP) of the fractions. Figure from Leppä et al. (III).

### 3.4.2 Plant-by-plant comparison

Figure 21 shows the plant species specific anthelmintic activities as a function of mDP (III). Figure 21A shows that the highest IA-% was measured for *P. Sylvestris* (IA-% = 88–99%), *S. phylicifolia* (IA-% = 50–93%), *L. vulgaris* (IA-% = 57–100%) and *T. repens* (IA-% = 67–99%). The same plant species were also efficient at the mortality assay, although *P. Sylvestris* (LM-% = 21–30%) and *S. phylicifolia* (LM-% = 15–28%) were significantly more efficient than *L. vulgaris* (LM-% = 10–18%) and *T. repens* (LM-% = 15–23%) (Figure 21B). The fractions of *T. repens* were extremely PD-% rich (PD-% = 76–99%) while the variation in PD-% was greater in *P. Sylvestris* (PD-% = 47–85%), *S. phylicifolia* (PD-% = 8–93%) and *L. vulgaris* (PD-% = 30–92%). The mDP of these plants were mDP = 11–30; 14–27; 14–25 and 11–39, respectively. In general, the isolated fractions of these plant species had a high mDP and contained PD units at least to some extent.

On average, slightly lower activities were measured for *Larix* sp., *L. corniculatus* and *R. alpinum*, whose inhibitory activities were IA-% = 58–86%; 57–100% and 56–82% and mortalities LM-% = 1–16%; 12–44% and 3–13%, respectively. The most likely explanation is their lower mDPs (mDP = 9–14; 10–21 and 11–25,

respectively) as compared to the most active plant species described in the previous paragraph.

The plant species with the lowest activities were galloylated *R. dichroanthum* and *R. schlippenbachii* and very PC rich *T. medium* and *A. hippocastanum* (Figure 21). Their inhibitory activity was clearly lower (IA-% = 0–75%) than in other plant species and their mortality was rather low (LM-% = 0–15%) as well. One explanation for the low activity of these plant species could be their lower mDP (<10, Figure 21) or PD-% (0–40%, Figure S3 in **III**) as compared to the rest of the plant species. Previous studies have shown, that the galloylation of the flavan-3-ol subunits increases the anthelmintic activity<sup>99</sup>, which was not observed herein. Possible explanation for this could be the low galloyl content of the *R. dichroanthum* and *R. schlippenbachii* fractions, which was <1 (mol/mol) in the majority of the fractions (see Figure S7 in **III**).

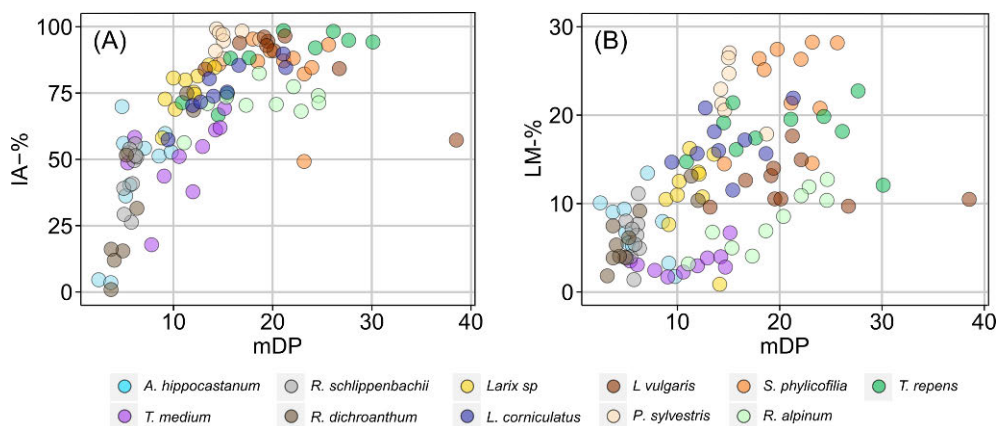


Figure 21. (A) Migration inhibition activity (IA-%) and (B) larval mortality (LM-%) of the studied samples as a function of the mean degree of polymerisation (mDP). The plant species are illustrated with different colours. Figure from Leppä et al (**III**).

The low activity was not solely caused by low mDP. For instance, Figure 21B shows that the *T. medium* fractions had lower mortality (LM-% = 2–7%) in comparison to *A. hippocastanum* (LM-% = 2–14%) while the mDP of the *T. medium* fractions was clearly higher. Both plants were also extremely rich in PC (*T. medium* PD-% = 1%, *A. hippocastanum* PD-% = 1%). One possible explanation for this difference in activity could be the substantially higher composition of A-type PCs in *A. hippocastanum* as compared to *T. medium* (see Figures S9 and S10 in **III**). The A-type bond between flavan-3-ol units alters the flexibility and water solubility of the molecule thus affecting the interaction with proteins.<sup>2</sup> In previous studies, the A-type PAs have shown greater affinity towards proteins than B-type PAs.<sup>60</sup> This finding

supports the previous hypothesis that the anthelmintic activities of PAs are caused by their tendency to form complexes with proteins.<sup>87</sup>

### 3.4.3 Linkage between protein precipitation capacity and anthelmintic activity

Lastly, the estimated PPC values of each fraction was calculated based on the plant species specific PLSR equations with the non-standardised regression coefficients (Table S2 in II) and the estimated PPC values were mapped against hereby measured anthelmintic activity values (Figure 22). Both scatter plots resemble the previously shown Figure 19, where the activities were plotted against mDP. The IA-% increased logarithmically ( $y = -165 + 29 \times \ln(x)$ ,  $R^2 = 0.61$ , Figure 22A) and the LM-% increased linearly ( $y = 7.54 + 0.0012x$ ,  $R^2 = 0.17$ , Figure 22B) as a function of the estimated PPC with the used PA concentration. The correlation between mortality and estimated PPC was clear yet weak ( $R^2 = 0.17$ ).

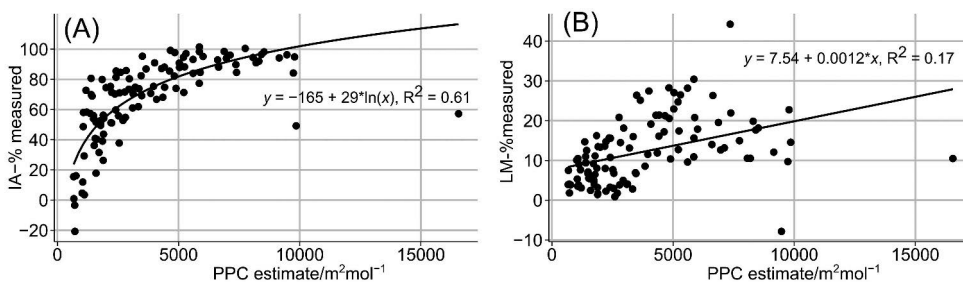


**Figure 22.** Measured (A) migration inhibition activity (IA-%), and (B) larval mortality (LM-%) as a function of the estimated protein precipitation capacity (PPC).

Previous studies have suggested that the anthelmintic activity mechanisms might act through complex formation between PAs and proteins.<sup>87</sup> The fact that similar structural features, such as large polymer size seem to increase both anthelmintic activity<sup>89,90</sup> and protein binding<sup>56</sup> has been the primary argument supporting this hypothesis. Also our results supported this theory even though, our approach focused on measuring the amount of precipitated complexes (II). The formation of insoluble complexes is not the same as binding proteins, but they are merely the different stages of the same phenomenon.<sup>61</sup> Also, other studies have shown the increase in the formation of insoluble complexes with high mDP<sup>55,57</sup>. Our results are in good accordance with the literature and further support the above described hypothesis about the mode of action.

### 3.5 Ensiling of *Vicia faba*

In the comparison of different ensiling processes of *Vicia faba* seeds, the concentration of both soluble and insoluble PAs decreased during the ensiling process (see Table 5, in **IV**). After ensiling, the amount of remaining total PAs ranged between 33% and 94% and soluble PAs from 0% to 17%. The decrease was greatest in the salt treated seeds, where no traces of soluble PAs were found after ensiling and the amount of total PA was 33% from the original PA composition. The amount of total PAs in crimped faba bean was 10.9 g/kg dry matter (DM), out of which 3.1 g/kg DM were soluble PAs. The amount of total PAs after treatment varied from 3.6 to 10.3 g/kg DM, whilst the soluble PAs ranged from 0.0 to 0.54 g/kg DM. The PD-% from the total PA fingerprint in crimped faba bean was PD-% = 69.9% (Table 2, in **IV**), which remained fairly stable in other treatments (PD-% = 68.3–73.0%) except for salt (PD-% = 63.5%). The PD-% in the soluble PA fingerprint (PD-% = 64.9%) decreased slightly after ensiling (PD-% = 57.3–61.3%). The mDP of the soluble PAs decreased from 9.3 to 6.0–6.8 after ensiling. These observations show, that some structural features or chemical properties of PAs increase their probability to either form insoluble complexes with protein or fibre and thus be unavailable for extraction and analysis or degrade completely.<sup>101,108</sup> Such features were for instance high mDP and PD structural units.

The PA fingerprints remained rather similar after ensiling, except for a PC terminal unit peak at  $t_R = 4.2$  min, which emerged in all ensiled samples (Figure 23, B–H). The reason for this might be that, the small PC oligomers are more resistant to degradation or transforming into non extractable form. Other possible explanation could be that these small oligomers could be the degradation products of larger oligomers. The profiles of the PA fingerprints (Figure 23) remained rather similar after ensiling except for the salt treated seeds. This suggests that apart from the salt treated seeds, there were no drastic changes in the PC/PD composition of *Vicia faba* seeds. (**IV**)

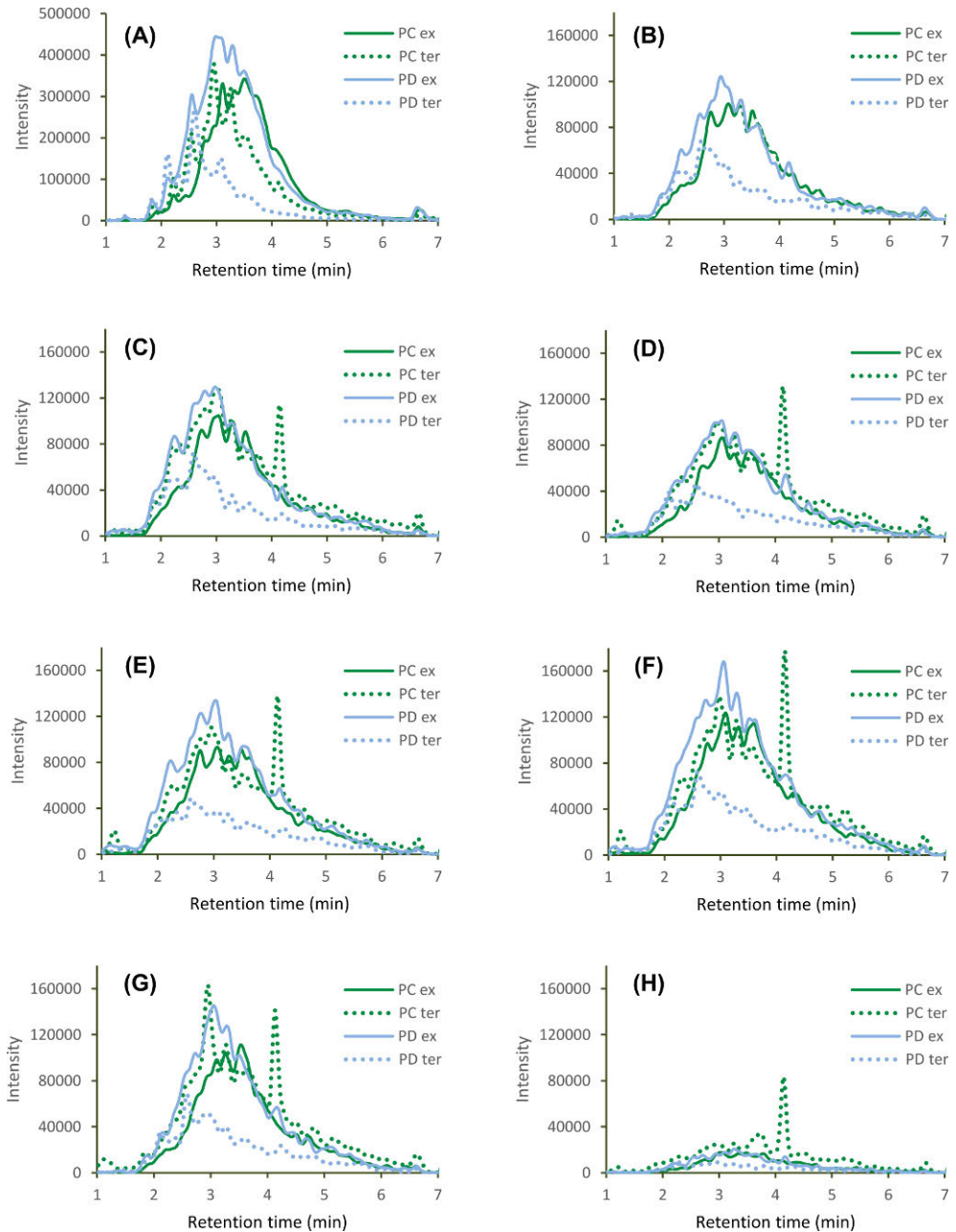


**Figure 23.** Multiple reaction monitoring traces of faba bean samples (A) before ensiling, (B) control, (C) control + water, (D) LABmix, (E) LABmix + water, (F) LABLuke, (G) formic acid and (H) salt. The abbreviations are as follows PC ex, procyanidin extension unit; PC ter, procyanidin terminal unit; PD ex, prodelphinidin extension unit; and PD ter, prodelphinidin terminal unit. Figure from Rinne et al. (IV).

## 4 Conclusions

The semipreparative fractionation of PAs showed, that it was possible to obtain PA rich sub-fractions, which were drastically different from the composition of the original PA material. UPLC-MS/MS results showed that the mDP, PD-% and the retention time window of the PA rich sub-fractions differed significantly from the original PA composition. The more detailed examination of the PA composition via HRMS data verified these findings. Even such sub-fractions, which were isolated from the same plant material, contained completely different PA molecular composition.

The protein precipitation capacity studies of these fractions highlighted the importance of polymer size to the PPC. Other structural features were important from the protein precipitation point of view as well, but the relevance of different factors differed significantly amongst tested plant species. The distribution of PPC within PA fingerprints was more consistent in those plant species, which were extremely rich in either PC or PD units. In such plant species, which contained a more heterogeneous mixture of PC and PC, the distribution of PPC was rather irregular.

The anthelmintic activity measurement gave rather similar results as was obtained with the PPC study. The most significant structural feature of PAs increasing their anthelmintic activity were mDP and PD-%. In PC rich plant species, the A-type linkage between the flavan-3-ol units increased the activity substantially. Due to the similarities of both protein precipitation and anthelmintic activity results, these studies supported the hypothesis that the anthelmintic activities of PAs are caused by their interaction with proteins.

The combination of highly refined PA fractions, accurate analytical tools and afore-described bioactivity assays offered bioactivity–structure relationship information in such detail, which has not been possible earlier. For instance, the distribution of protein precipitation capacity was analysed in different parts of the PA fingerprint, revealing which part of the fingerprint was active in each plant species. Also, the anthelmintic activity study showed that from both PC rich plant species of this study (*A. hippocastanum* and *T. medium*) the one, which contained mainly A-type PAs (*A. hippocastanum*) was substantially more active than the one containing more B-type PAs (*T. medium*). Without the use of accurate mass

spectrometric measurements, the compound specific information of the studied fractions would have stayed unravelled. Therefore, the combination of methods utilised herein was crucial for the accuracy and high-quality of the results.

Finally, the ensiling experiments of *Vicia faba* showed that the concentration of total and soluble PAs decreased after ensiling. The decrease was the most significant in salt treated *Vicia faba*, where no traces of soluble PAs were found after ensiling. Possible explanations for the decrease in PA concentration were suggested to be due to the degradation of PAs or their transformation into non-soluble form. The knowledge of the fate of these compounds is crucial for the possible future utilisations of bioactive feeds as potent nutraceuticals.

The results of this work offer highly useful information about the bioactivity–structure relationships of PAs as well as tools for the purification of these compounds. The results also support previously suggested hypothesis about the possible mode of action behind anthelmintic activity of PAs. Even though many questions were answered during this project, some new questions still emerged. For instance, anthelmintic activity and protein precipitation behaviour of galloylated PAs were not consistent or in accordance with previous literature. Further studies with more focused set of PAs could perhaps offer the answer. All in all, the bioactivity–structure interactions of PAs still remain as highly complex field of research area, where the interdisciplinary collaboration offers insightful new approaches and solutions to the complex dilemmas.

# Acknowledgements

The work of this PhD project was mainly carried out in the Laboratory of Organic Chemistry and Chemical Biology at the Department of Chemistry, University of Turku since 2016. Partially, this work was also executed in the Laboratory of Parasites, Immunology and Gut Health (PIGH) in the section of Parasitology and Aquatic Pathobiology in Department of Veterinary and Animal Sciences in the University of Copenhagen. The paper about *Vicia faba* was carried out in collaboration with Natural Resource Institute of Finland (LUKE). I wish to acknowledge the co-authors of this paper and special thanks go to Professor Marketta Rinne. The following funding sources are gratefully acknowledged for enabling me the possibility to work full-time with this project: Raisio Research Foundation, Academy of Finland (grant number 298177), Finnish Cultural Foundation and Satakunta Regional Fund.

This PhD has been thus far, the most demanding yet rewarding project I have ever taken part in. I have learned how scientific research is done, met the most amazing people and learned a thing or two about myself. In addition to my own papers and studies, I have also gotten the opportunity to supervise Master and Bachelor students in our laboratory and learn from these experiences.

I wish to express my gratitude to Professor María Teresa Escribano-Bailón and Dr. Sylvain Guyot for pre-examining and evaluating my thesis and Professor emerita Riitta Julkunen-Tiitto for taking up the task of being my opponent in these special circumstances.

My deepest gratitude goes to my Professor Juha-Pekka Salminen. Under your patient guidance, I had the time to search my inner scientist and whenever needed, you gave a gentle push forward. When I started, I probably was one of those students, who needed a quite a lot of support, but gradually my independence and courage grew. You have always encouraged keeping my head in such situations, where I have hesitated and for me, that was truly invaluable. In addition to the help and support in chemistry related and other professional issues, we also shared similar sense of humour probably thanks to our Satakunta backgrounds...

My other supervisors Docent Maarit Karonen, Docent Petri Tähtinen and Dr. Marica Engström were absolutely irreplaceable for my journey to a PhD. Maarit, your expertise in the mass spectrometry related issues especially in the beginning of

this project was crucial for the first paper. Over time, your support slowly shifted from the professional issues more into personal aspects of life. Petri, you were always present in the meeting and anytime really. You gave the most sharp-eyed comments of my manuscripts and the thesis itself. Marica, you joined to my supervisor group while this project was already ongoing. I could not be happier that you decided take up this duty. Your friendship and support helped greatly during these years.

I have been enormously lucky and in spring 2019 I got the opportunity to fulfil my dream to work abroad. I visited the Laboratory of Parasites, Immunology and Gut Health (PIGH) in the University of Copenhagen, Denmark. During that time, I was kindly supervised by Associate Professor Andrew R. Williams to whom I am very grateful. I felt instantly welcomed to the group and I want to express my gratitude to everyone who made my time in Denmark memorable. Special thanks go to my roommates Ling Zhu and Dr. Laura Myhill, Mette Marie Schjelde, Charlotte Bonde, Angela Valente, Leah Lourenco, Professor Stig M. Thamsborg and of course, Audrey Inge Andersen-Civil.

I wish to thank Kirsi Laaksonen, Mauri Nauma and Kari Loikas for all the help in chemical, IT and hardware related issues.

During this nearly 5-year journey to a PhD, I have been a part of the most amazing research group (Natural Chemistry Research Group, NCRG). I have always felt like home working here and that is all thanks to the group members. Thank you for all the conference trips, coffee breaks, lab tips and shared laughs Suvi Vanhakylä, Jussi Suvanto, Jorma Kim, Iqbal Bin Imran, Valtteri Virtanen, Ilari Kuukkanen, Mimosa Sillanpää and Anne Koivuniemi. Special thanks go to my roommate Marianna Manninen. I will miss our profound discussions. I want to also thank the former PhD students and group members of NCRG Sanjib Saha, Dr. Nicolas Baert, Dr. Anu Tuominen, Dr. Elina Puljula, and Kaija-Liisa Laine for the enjoyable working atmosphere.

Life is not all about work and especially for me, the frequent visits at the stables were crucial for my well-being. I want to thank the amazing people and horses of Ratsutalli Friskala for the much-needed breaks from the academic world. Special thanks go to Minna Lehtonen, Kirsi Udelius, Marjo Nurmisto, Dr. Sini Eloranta, Heli Ylä-Outinen, Katariina Nordell, Joakim Alander, Henna Kivilä and Päivi Savilahti-Bäckman.

I was fortunate to start my studies at the University with my dear friends Tiina Jaakkola, Saku Valkamaa, Marika Valkamaa, Annika Lehtimäki, Anna-Leena Hakoila, and Mia Meriläinen. Thank you for the undergraduate years and everything that came along. Thank you for the company in the morning lectures, shared confusion in the laboratory, drowsy lecture breaks in the Arcanum lobby, long walks home after a night out, and everything else. We have shared together the big

Milla Leppä

moments of our lives (graduations, engagements, weddings, babies...) and I hope, there is no end in sight. Simply put, thank you for your friendship.

I want to thank my friends Eveliina Äärelä, Sini Aaltonen, Antti Äärelä and Sampo Hirvioja for your friendship during these years. Thank you for all the good moments, Christmas parades, Independence Day celebrations and your support on the rough patches.

I wish to thank to my parents Marja and Reima Leppä, my brothers Ville and Matti Leppä and my grandmothers Vappu Hakala and Liisa Leppä for your endless support. I also want to thank Kaisa Mursu, Kari Laitila, Jutta Laitila, and Jenna Laitila. Finally, I want to thank my muru Juuso Laitila for everything. Everything. You know what it means.

15.11.2020



# References

- (1) Haslam, E. *Practical Polyphenolics: From Structure to Molecular Recognition and Physiological Action*; Cambridge Univ. Press: Cambridge, 1998.
- (2) Zeller, W. E. Activity, Purification, and Analysis of Condensed Tannins: Current State of Affairs and Future Endeavors. *Crop Sci.* **2019**, *59* (3), 886–904. <https://doi.org/10.2135/cropsci2018.05.0323>.
- (3) Lin, L. Z.; Sun, J.; Chen, P.; Monagas, M. J.; Harnly, J. M. UHPLC-PDA-ESI/HRMS<sup>n</sup> Profiling Method to Identify and Quantify Oligomeric Proanthocyanidins in Plant Products. *J. Agric. Food Chem.* **2014**, *62* (39), 9387–9400. <https://doi.org/10.1021/jf501011y>.
- (4) Hayasaka, Y.; Waters, E. J.; Cheynier, V.; Herderich, M. J.; Vidal, S. Characterization of Proanthocyanidins in Grape Seeds Using Electrospray Mass Spectrometry. *Rapid Commun. Mass Spectrom.* **2003**, *17* (1), 9–16. <https://doi.org/10.1002/rem.869>.
- (5) Gu, L.; Kelm, M. A.; Hammerstone, J. F.; Beecher, G.; Holden, J.; Haytowitz, D.; Prior, R. L. Screening of Foods Containing Proanthocyanidins and Their Structural Characterization Using LC-MS/MS and Thiolytic Degradation. *J. Agric. Food Chem.* **2003**, *51* (23), 7513–7521. <https://doi.org/10.1021/jf034815d>.
- (6) Ettre, L. S. Nomenclature for Chromatography (IUPAC Recommendations 1993). *Pure Appl. Chem.* **1993**, *65* (4), 819–872. <https://doi.org/10.1351/pac199365040819>.
- (7) Fischer, N.; Weinreich, B.; Nitz, S.; Drawert, F. Applications of High-Speed Counter-Current Chromatography for the Separation and Isolation of Natural Products. *J. Chromatogr., A* **1991**, *538* (1), 193–202. [https://doi.org/10.1016/S0021-9673\(01\)91637-1](https://doi.org/10.1016/S0021-9673(01)91637-1).
- (8) Luca, S. V.; Bujor, A.; Miron, A.; Aprotosoaic, A. C.; Skalicka-Woźniak, K.; Trifan, A. Preparative Separation and Bioactivity of Oligomeric Proanthocyanidins. *Phytochem. Rev.* **2019**, *5*. <https://doi.org/10.1007/s11101-019-09611-5>.
- (9) Saminathan, M.; Tan, H. Y.; Sico, C. C.; Abdullah, N.; Wong, C. M. V. L.; Abdulmalek, E.; Ho, Y. W. Polymerization Degrees, Molecular Weights and Protein-Binding Affinities of Condensed Tannin Fractions from a *Leucaena Leucocephala* Hybrid. *Molecules* **2014**, *19* (6), 7990–8010. <https://doi.org/10.3390/molecules19067990>.
- (10) Brown, R. H.; Mueller-harvey, I.; Zeller, W. E.; Reinhardt, L.; Stringano, E.; Gea, A.; Drake, C.; Ropiak, H. M.; Fryganas, C.; Ramsay, A.; Hardcastle, E. E.. Facile Purification of Milligram to Gram Quantities of Condensed Tannins According to Mean Degree of Polymerization and Flavan-3-Ol Subunit Composition. *J. Agric. Food Chem.* **2017**, *65* (36), 8072–8082. <https://doi.org/10.1021/acs.jafc.7b03489>.
- (11) Guadalupe, Z.; Soldevilla, A.; Sáenz-Navajas, M. P.; Ayestarán, B. Analysis of Polymeric Phenolics in Red Wines Using Different Techniques Combined with Gel Permeation Chromatography Fractionation. *J. Chromatogr., A* **2006**, *1112*, 112–120. <https://doi.org/10.1016/j.chroma.2005.11.100>.
- (12) Yanagida, A.; Shoji, T.; Shibusawa, Y. Separation of Proanthocyanidins by Degree of Polymerization by Means of Size-Exclusion Chromatography and Related Techniques. *J. Biochem. Biophys. Methods* **2003**, *56*, 311–322. [https://doi.org/10.1016/S0165-022X\(03\)00068-X](https://doi.org/10.1016/S0165-022X(03)00068-X).

- (13) Salminen, J.-P.; Karonen, M.; Sinkkonen, J. Chemical Ecology of Tannins: Recent Developments in Tannin Chemistry Reveal New Structures and Structure-Activity Patterns. *Chem. - Eur. J.* **2011**, *17* (10), 2806–2816. <https://doi.org/10.1002/chem.201002662>.
- (14) Jiang, G.; Du, F.; Fang, G. Two New Proanthocyanidins from the Leaves of *Garcinia Multiflora*. *Natural Product Research*. Taylor & Francis 2014, pp 449–453. <https://doi.org/10.1080/14786419.2013.873431>.
- (15) Oldoni, T. L. C.; Melo, P. S.; Massarioli, A. P.; Moreno, I. A. M.; Bezerra, R. M. N.; Rosalen, P. L.; Da Silva, G. V. J.; Nascimento, A. M.; Alencar, S. M. Bioassay-Guided Isolation of Proanthocyanidins with Antioxidant Activity from Peanut (*Arachis Hypogaea*) Skin by Combination of Chromatography Techniques. *Food Chem.* **2016**, *192*, 306–312. <https://doi.org/10.1016/j.foodchem.2015.07.004>.
- (16) McMurrough, I.; Madigan, D.; Smyth, M. R. Semipreparative Chromatographic Procedure for the Isolation of Dimeric and Trimeric Proanthocyanidins from Barley. *J. Agric. Food Chem.* **1996**, *44* (7), 1731–1735. <https://doi.org/10.1021/jf960139m>.
- (17) Hellström, J.; Sinkkonen, J.; Karonen, M.; Mattila, P. Isolation and Structure Elucidation of Procyanidin Oligomers from Saskatoon Berries (*Amelanchier Alnifolia*). *J. Agric. Food Chem.* **2007**, *55*, 157–164. <https://doi.org/10.1021/jf062441t>
- (18) Appeldoorn, M. M.; Sanders, M.; Vincken, J.-P.; Cheynier, V.; Le Guernevé, C.; Hollman, P. C. H.; Gruppen, H. Efficient Isolation of Major Procyanidin A-Type Dimers from Peanut Skins and B-Type Dimers from Grape Seeds. *Food Chem.* **2009**, *117*, 713–720. <https://doi.org/10.1016/j.foodchem.2009.04.047>.
- (19) Karonen, M.; Lopenen, J.; Ossipov, V.; Pihlaja, K. Analysis of Procyanidins in Pine Bark with Reversed-Phase and Normal-Phase High-Performance Liquid Chromatography-Electrospray Ionization Mass Spectrometry. *Anal. Chim. Acta* **2004**, *522* (1), 105–112. <https://doi.org/10.1016/j.aca.2004.06.041>.
- (20) Zumdick, S.; Petereit, F.; Luftmann, H.; Hensel, A. Preparative Isolation of Oligomeric Procyanidins from Hawthorn (*Crataegus* Spp.). *Pharmazie* **2009**, *64* (4), 286–288. <https://doi.org/10.1691/ph.2009.8794>.
- (21) Kelm, M. A.; Johnson, J. C.; Robbins, R. J.; Hammerstone, J. F.; Schmitz, H. H. High-Performance Liquid Chromatography Separation and Purification of Cacao (*Theobroma cacao* L.) Procyanidins According to Degree of Polymerization Using a Diol Stationary Phase. *J. Agric. Food Chem.* **2006**, *54* (5), 1571–1576. <https://doi.org/10.1021/jf0525941>.
- (22) Berthod, A.; Maryutina, T.; Spivakov, B.; Shpigun, O.; Sutherland, I. A. Countercurrent Chromatography in Analytical Chemistry (IUPAC Technical Report). *Pure Appl. Chem.* **2009**, *81* (2), 355–387. <https://doi.org/10.1351/PAC-REP-08-06-05>.
- (23) Liu, Y.; Friesen, J. B.; McAlpine, J. B.; Pauli, G. F. Solvent System Selection Strategies in Countercurrent Separation. *Planta Med.* **2015**, *81* (17), 1582–1591. <https://doi.org/10.1055/s-0035-1546246>.
- (24) Sumner, N. Developing Counter Current Chromatography to Meet the Needs of Pharmaceutical Discovery. *J. Chromatogr., A* **2011**, *1218* (36), 6107–6113. <https://doi.org/10.1016/j.chroma.2011.05.001>.
- (25) Putman, L. J.; Butler, L. G. Fractionation of Condensed Tannins by Counter-Current Chromatography. *J. Chromatogr., A* **1985**, *318* (C), 85–93. [https://doi.org/10.1016/S0021-9673\(01\)90666-1](https://doi.org/10.1016/S0021-9673(01)90666-1).
- (26) Esatbeyoglu, T.; Winterhalter, P. Preparation of Dimeric Procyanidins B1, B2, B5, and B7 from a Polymeric Procyanidin Fraction of Black Chokeberry (*Aronia Melanocarpa*). *J. Agric. Food Chem.* **2010**, *58* (8), 5147–5153. <https://doi.org/10.1021/jf904354n>.
- (27) Esatbeyoglu, T.; Wray, V.; Winterhalter, P. Isolation of Dimeric, Trimeric, Tetrameric and Pentameric Procyanidins from Unroasted Cocoa Beans (*Theobroma Cacao* L.) Using Countercurrent Chromatography. *Food Chem.* **2015**, *179*, 278–289. <https://doi.org/10.1016/j.foodchem.2015.01.130>.

- (28) Guyot, S.; Doco, T.; Souquet, J. M.; Moutounet, M.; Drilleau, J.-F. Characterization of Highly Polymerized Procyanidins in Cider Apple (*Malus Sylvestris* Var. Kermerrien) Skin and Pulp. *Phytochemistry* **1997**, *44* (2), 351–357. [https://doi.org/10.1016/S0031-9422\(96\)00480-3](https://doi.org/10.1016/S0031-9422(96)00480-3).
- (29) Engström, M. T.; Päljjarvi, M.; Fryganas, C.; Grabber, J. H.; Mueller-Harvey, I.; Salminen, J.-P. Rapid Qualitative and Quantitative Analyses of Proanthocyanidin Oligomers and Polymers by UPLC-MS/MS. *J. Agric. Food Chem.* **2014**, *62* (15), 3390–3399. <https://doi.org/10.1021/jf500745y>.
- (30) Engström, M. T.; Päljjarvi, M.; Salminen, J.-P. Rapid Fingerprint Analysis of Plant Extracts for Ellagitannins, Gallic Acid, and Quinic Acid Derivatives and Quercetin-, Kaempferol- and Myricetin-Based Flavonol Glycosides by UPLC-QqQ-MS/MS. *J. Agric. Food Chem.* **2015**, *63* (16), 4068–4079. <https://doi.org/10.1021/acs.jafc.5b00595>.
- (31) Karas, M.; Bachmann, D.; Bahr, U.; Hillenkamp, F. Matrix-Assisted Ultraviolet Laser Desorption of Non-Volatile Compounds. *Int. J. Mass Spectrom.* **1987**, *78*, 53–68. [https://doi.org/10.1016/0168-1176\(87\)87041-6](https://doi.org/10.1016/0168-1176(87)87041-6).
- (32) Chai, W.-M.; Shi, Y.; Feng, H.-L.; Qiu, L.; Zhou, H.-C.; Deng, Z.-W.; Yan, C.-L.; Chen, Q.-X. NMR, HPLC-ESI-MS, and MALDI-TOF MS Analysis of Condensed Tannins from *Delonix Regia* (Bojer Ex Hook.) Raf. and Their Bioactivities. *J. Agric. Food Chem.* **2012**, *60* (19), 5013–5022. <https://doi.org/10.1021/jf300740d>.
- (33) Mane, C.; Sommerer, N.; Yalcin, T.; Cheynier, V.; Cole, R. B.; Fulcrand, H. Assessment of the Molecular Weight Distribution of Tannin Fractions through MALDI-TOF MS Analysis of Protein–Tannin Complexes. *Anal. Chem.* **2007**, *79* (6), 2239–2248. <https://doi.org/10.1021/ac061685>.
- (34) Perez-Gregorio, M. R.; Mateus, N.; de Freitas, V. Rapid Screening and Identification of New Soluble Tannin-Salivary Protein Aggregates in Saliva by Mass Spectrometry (MALDI-TOF-TOF and FIA-ESI-MS). *Langmuir* **2014**, *30* (28), 8528–8537. <https://doi.org/10.1021/la502184f>.
- (35) Engström, M. T.; Sun, X.; Suber, M. P.; Li, M.; Salminen, J.-P.; Hagerman, A. E. The Oxidative Activity of Ellagitannins Dictates Their Tendency To Form Highly Stabilized Complexes with Bovine Serum Albumin at Increased pH. *J. Agric. Food Chem.* **2016**, *64* (47), 8994–9003. <https://doi.org/10.1021/acs.jafc.6b01571>.
- (36) Gu, L.; Kelm, M. A.; Hammerstone, J. F.; Zhang, Z.; Beecher, G.; Holden, J.; Haytowitz, D.; Prior, R. L. Liquid Chromatographic/Electrospray Ionization Mass Spectrometric Studies of Proanthocyanidins in Foods. *J. Mass Spectrom.* **2003**, *38* (12), 1272–1280. <https://doi.org/10.1002/jms.541>.
- (37) Karonen, M.; Liimatainen, J.; Sinkkonen, J. Birch Inner Bark Procyanidins Can Be Resolved with Enhanced Sensitivity by Hydrophilic Interaction HPLC-MS. *J. Sep. Sci.* **2011**, *34* (22), 3158–3165. <https://doi.org/10.1002/jssc.201100569>.
- (38) Giribaldi, J.; Besson, M.; Suc, L.; Fulcrand, H.; Mouis, L. The Use of Extracted-Ion Chromatograms to Quantify the Composition of Condensed Tannin Subunits. *Rapid Commun. Mass Spectrom.* **2020**, *34* (7), 1–10. <https://doi.org/10.1002/rcm.8619>.
- (39) Mouis, L.; Mazauric, J.-P.; Sommerer, N.; Fulcrand, H.; Mazerolles, G. Comprehensive Study of Condensed Tannins by ESI Mass Spectrometry: Average Degree of Polymerisation and Polymer Distribution Determination from Mass Spectra. *Anal. Bioanal. Chem.* **2011**, *400* (2), 613–623. <https://doi.org/10.1007/s00216-011-4751-7>.
- (40) Murray, K. K.; Boyd, R. K.; Eberlin, M. N.; John Langley, G.; Li, L.; Naito, Y. Definitions of Terms Relating to Mass Spectrometry (IUPAC Recommendations 2013). *Pure Appl. Chem.* **2013**, *85* (7), 1515–1609. <https://doi.org/10.1351/PAC-REC-06-04-06>.
- (41) Ropiak, H. M.; Ramsay, A.; Mueller-Harvey, I. Condensed Tannins in Extracts from European Medicinal Plants and Herbal Products. *J. Pharm. Biomed. Anal.* **2016**, *121*, 225–231. <https://doi.org/10.1016/j.jpba.2015.12.034>.

- (42) Howell, A. B.; Reed, J. D.; Krueger, C. G.; Winterbottom, R.; Cunningham, D. G.; Leahy, M. A. Type Cranberry Proanthocyanidins and Uropathogenic Bacterial Anti-Adhesion Activity. *Phytochemistry* **2005**, *66*, 2281–2291. <https://doi.org/10.1016/j.phytochem.2005.05.022>.
- (43) Salminen, J.-P.; Karonen, M.; Lempa, K.; Liimatainen, J.; Sinkkonen, J.; Lukkarinen, M.; Pihlaja, K. Characterisation of Proanthocyanidin Aglycones and Glycosides from Rose Hips by High-Performance Liquid Chromatography-Mass Spectrometry, and Their Rapid Quantification Together with Vitamin C. *J. Chromatogr., A* **2005**, *1077* (2), 170–180. <https://doi.org/10.1016/j.chroma.2005.04.073>.
- (44) Kennedy, J. A.; Jones, G. P. Analysis of Proanthocyanidin Cleavage Products Following Acid-Catalysis in the Presence of Excess Phloroglucinol. *J. Agric. Food Chem.* **2001**, *49* (4), 1740–1746. <https://doi.org/10.1021/jf001030o>.
- (45) Kennedy, J. A.; Taylor, A. W. Analysis of Proanthocyanidins by High-Performance Gel Permeation Chromatography. *J. Chromatogr., A* **2003**, *995*, 99–107. [https://doi.org/https://doi.org/10.1016/S0021-9673\(03\)00420-5](https://doi.org/https://doi.org/10.1016/S0021-9673(03)00420-5).
- (46) Desrués, O.; Peña-Espinoza, M.; Hansen, T. V. A.; Enemark, H. L.; Thamsborg, S. M. Anti-Parasitic Activity of Pelleted Sainfoin (*Onobrychis Viciifolia*) against *Ostertagia Ostertagi* and *Cooperia Oncophora* in Calves. *Parasites and Vectors* **2016**, *9* (1), 1–10. <https://doi.org/10.1186/s13071-016-1617-z>.
- (47) Girard, M.; Dohme-Meier, F.; Wechsler, D.; Goy, D.; Kreuzer, M.; Bee, G. Ability of 3 Tanniferous Forage Legumes to Modify Quality of Milk and Gruyère-Type Cheese. *J. Dairy Sci.* **2016**, *99* (1), 205–220. <https://doi.org/10.3168/jds.2015-9952>.
- (48) Bee, G.; Dohme-Meier, F.; Girard, M. The Potential of Condensed Tannin-Rich Feedstuff to Affect the Nutritional and Sensory Qualities of Ruminant-Based Products. *IOP Conf. Ser. Earth Environ. Sci.* **2019**, *333* (1). <https://doi.org/10.1088/1755-1315/333/1/012004>.
- (49) Girard, M.; Dohme-Meier, F.; Silacci, P.; Ampuero Kragten, S.; Kreuzer, M.; Bee, G. Forage Legumes Rich in Condensed Tannins May Increase N-3 Fatty Acid Levels and Sensory Quality of Lamb Meat. *J. Sci. Food Agric.* **2016**, *96* (6), 1923–1933. <https://doi.org/10.1002/jsfa.7298>.
- (50) Hatew, B.; Stringano, E.; Mueller-Harvey, I.; Hendriks, W. H.; Carbonero, C. H.; Smith, L. M. J.; Pellikaan, W. F. Impact of Variation in Structure of Condensed Tannins from Sainfoin (*Onobrychis Viciifolia*) on *in Vitro* Ruminant Methane Production and Fermentation Characteristics. *J. Anim. Physiol. Anim. Nutr.* **2016**, *100* (2), 348–360. <https://doi.org/10.1111/jpn.12336>.
- (51) Engström, M. T.; Arvola, J.; Nenonen, S.; Virtanen, V. T. J.; Leppä, M. M.; Tähtinen, P.; Salminen, J.-P. Structural Features of Hydrolyzable Tannins Determine Their Ability to Form Insoluble Complexes with Bovine Serum Albumin. *J. Agric. Food Chem.* **2019**, *67* (24), 6798–6808. <https://doi.org/10.1021/acs.jafc.9b02188>.
- (52) Oh, H.; Hoff, J. E.; Armstrong, G. S.; Haff, L. A. Hydrophobic Interaction in Tannin-Protein Complexes. *J. Agric. Food Chem.* **1980**, *28*, 394–398. <https://doi.org/10.1021/jf60228a020>.
- (53) Hagerman, A. E.; Butler, L. G. Condensed Tannin Purification and Characterization of Tannin-Associated Proteins. *J. Agric. Food Chem.* **1980**, *28* (5), 947–952. <https://doi.org/10.1021/jf60231a011>.
- (54) Hagerman, A. E.; Rice, M. E.; Ritchard, N. T. Mechanisms of Protein Precipitation for Two Tannins, Pentagalloyl Glucose and Epicatechin<sub>16</sub> (4→8) Catechin (Procyanidin). *J. Agric. Food Chem.* **1998**, *46*, 2590–2595. <https://doi.org/10.1021/jf971097k>.
- (55) Zeller, W. E.; Sullivan, M. L.; Mueller-Harvey, I.; Grabber, J. H.; Ramsay, A.; Drake, C.; Brown, R. H. Protein Precipitation Behavior of Condensed Tannins from *Lotus Pedunculatus* and *Trifolium Repens* with Different Mean Degrees of Polymerization. *J. Agric. Food Chem.* **2015**, *63* (4), 1160–1168. <https://doi.org/10.1021/jf504715p>.
- (56) Kilmister, R. L.; Faulkner, P.; Downey, M. O.; Darby, S. J.; Falconer, R. J. The Complexity of Condensed Tannin Binding to Bovine Serum Albumin - An Isothermal Titration Calorimetry Study. *Food Chem.* **2016**, *190*, 173–178. <https://doi.org/10.1016/j.foodchem.2015.04.144>.

- (57) Ropiak, H. M.; Lachmann, P.; Ramsay, A.; Green, R. J.; Mueller-Harvey, I. Identification of Structural Features of Condensed Tannins That Affect Protein Aggregation. *PLoS One* **2017**, *12* (1). <https://doi.org/10.1371/journal.pone.0170768>.
- (58) Baxter, N. J.; Lilley, T. H.; Haslam, E.; Williamson, M. P. Multiple Interactions between Polyphenols and a Salivary Proline-Rich Protein Repeat Result in Complexation and Precipitation. *Biochemistry* **1997**, *36* (18), 5566–5577. <https://doi.org/10.1021/bi9700328>.
- (59) Cala, O.; Fouquet, E.; Laguerre, M.; Dufourc, E. J.; Pianet, I. NMR and Molecular Modeling of Wine Tannins Binding to Saliva Proteins : Revisiting Astringency from Molecular and Colloidal Prospects. *FASEB J.* **2010**, *24* (11), 4281–4290. <https://doi.org/10.1096/fj.10-158741>.
- (60) Zeller, W. E.; Reinhardt, L. A.; Robe, J. T.; Sullivan, M. L.; Panke-buisse, K. Comparison of Protein Precipitation Ability of Structurally Diverse Procyanidin-Rich Condensed Tannins in Two Buffer Systems. *J. Agric. Food Chem.* **2020**, *68* (7), 2016–2023. <https://doi.org/10.1021/acs.jafc.9b06173>.
- (61) Charlton, A. J.; Baxter, N. J.; Khan, M. L.; Moir, A. J. G.; Haslam, E.; Davies, A. P.; Williamson, M. P. Polyphenol/Peptide Binding and Precipitation. *J. Agric. Food Chem.* **2002**, *50* (6), 1593–1601. <https://doi.org/10.1021/jf010897z>.
- (62) Poncet-Legrand, C.; Edelmann, A.; Putax, J. L.; Cartalade, D.; Sarni-Manchado, P.; Vernhet, A. Poly(L-Proline) Interactions with Flavan-3-Ols Units: Influence of the Molecular Structure and the Polyphenol/Protein Ratio. *Food Hydrocolloids* **2006**, *20*, 687–697. <https://doi.org/https://doi.org/10.1016/j.foodhyd.2005.06.009>.
- (63) Lorenz, M. M.; Alkhafadji, L.; Stringano, E.; Nilsson, S.; Mueller-Harvey, I.; Udén, P. Relationship between Condensed Tannin Structures and Their Ability to Precipitate Feed Proteins in the Rumen. *J. Sci. Food Agric.* **2014**, *94* (5), 963–968. <https://doi.org/10.1002/jsfa.6344>.
- (64) de Freitas, V.; Carvalho, E.; Mateus, N. Study of Carbohydrate Influence on Protein-Tannin Aggregation by Nephelometry. *Food Chem.* **2003**, *81* (4), 503–509. [https://doi.org/10.1016/S0308-8146\(02\)00479-X](https://doi.org/10.1016/S0308-8146(02)00479-X).
- (65) Siebert, K. J.; Carrasco, A.; Lynn, P. Y. Formation of Protein-Polyphenol Haze in Beverages. *J. Agric. Food Chem.* **1996**, *44* (8), 1997–2005. <https://doi.org/10.1021/jf950716r>.
- (66) Hagerman, A. E.; Butler, L. G. The Specificity of Proanthocyanidin-Protein Interactions\*. *J. Biol. Chem.* **1981**, *256* (9), 4494–4497.
- (67) Roux, D. G. Molecular Weight of Condensed Tannins as a Factor Determining Their Affinity for Collagen. *Nature* **1958**, No. 4626, 1793–1794.
- (68) Osborne, N. J. T.; McNeill, D. M. Characterisation of Leucaena Condensed Tannins by Size and Protein Precipitation Capacity. *J. Sci. Food Agric.* **2001**, *81* (11), 1113–1119. <https://doi.org/10.1002/jsfa.920>.
- (69) Harbertson, J. F.; Kilmister, R. L.; Kelm, M. A.; Downey, M. O. Impact of Condensed Tannin Size as Individual and Mixed Polymers on Bovine Serum Albumin Precipitation. *Food Chem.* **2014**, *160*, 16–21. <https://doi.org/10.1016/j.foodchem.2014.03.026>.
- (70) Poncet-Legrand, C.; Gautier, C.; Cheyrier, V.; Imberty, A. Interactions between Flavan-3-Ols and Poly(L-Proline) Studied by Isothermal Titration Calorimetry: Effect of the Tannin Structure. *J. Agric. Food Chem.* **2007**, *55* (22), 9235–9240. <https://doi.org/https://doi.org/10.1021/jf071297o>.
- (71) Carvalho, E.; Mateus, N.; de Freitas, V. Flow Nephelometric Analysis of Protein-Tannin Interactions. *Anal. Chim. Acta* **2004**, *513* (1), 97–101. <https://doi.org/10.1016/j.aca.2003.10.010>.
- (72) Helsper, J. P. F. G.; Kolodziej, H.; Hoogendijk, J. M.; van Norel, A. Characterization and Trypsin Inhibitor Activity of Proanthocyanidins from *Vicia Faba*. *Phytochemistry* **1993**, *34* (5), 1255–1260. <https://doi.org/10.1055/s-2006-959978>.
- (73) Marmer, D. J.; Hurtubise, P. E. Nephelometric and Turbidimetric Immunoassay. In *Immunoassay*; Diamandis, E. P., Christopoulos, T. K., Eds.; Academic Press Inc., 1996; pp 363–387. <https://doi.org/10.1016/b978-012214730-2/50018-2>.

- (74) Dobрева, M. A.; Frazier, R. A.; Mueller-Harvey, I.; Clifton, L. A.; Gea, A.; Green, R. J. Binding of Pentagalloyl Glucose to Two Globular Proteins Occurs via Multiple Surface Sites. *Biomacromolecules* **2011**, *12* (3), 710–715. <https://doi.org/10.1021/bm101341s>.
- (75) Kaplan, R. M.; Vidyashankar, A. N. An Inconvenient Truth: Global Worming and Anthelmintic Resistance. *Vet. Parasitol.* **2012**, *186* (1–2), 70–78. <https://doi.org/10.1016/j.vetpar.2011.11.048>.
- (76) Charlier, J.; van der Voort, M.; Kenyon, F.; Skuce, P.; Vercruyse, J. Chasing Helminths and Their Economic Impact on Farmed Ruminants. *Trends Parasitol.* **2014**, *30* (7), 361–367. <https://doi.org/10.1016/j.pt.2014.04.009>.
- (77) Niezen, J.; Waghorn, G.; Charleston, W. A. Establishment and Fecundity of *Ostertagia circumcincta* and *Trichostrongylus colubriformis* in Lambs Fed Lotus (*Lotus pedunculatus*) or Perennial Ryegrass (*Lolium perenne*). *Vet. Parasitol.* **1998**, *78* (1), 13–21. [https://doi.org/10.1016/S0304-4017\(98\)00121-6](https://doi.org/10.1016/S0304-4017(98)00121-6).
- (78) Hoste, H.; Jackson, F.; Athanasiadou, S.; Thamsborg, S. M.; Hoskin, S. O. The Effects of Tannin-Rich Plants on Parasitic Nematodes in Ruminants. *Trends Parasitol.* **2006**, *22* (6), 253–261. <https://doi.org/10.1016/j.pt.2006.04.004>.
- (79) Athanasiadou, S.; Githiori, J.; Kyriazakis, I. Medicinal Plants for Helminth Parasite Control: Facts and Fiction. *Animal* **2007**, *1* (9), 1392–1400. <https://doi.org/10.1017/S1751731107000730>.
- (80) Engström, M. T.; Karonen, M.; Ahern, J. R.; Baert, N.; Payré, B.; Hoste, H.; Salminen, J.-P. Chemical Structures of Plant Hydrolyzable Tannins Reveal Their *in Vitro* Activity against Egg Hatching and Motility of *Haemonchus Contortus* Nematodes. *J. Agric. Food Chem.* **2016**, *64* (4), 840–851. <https://doi.org/10.1021/acs.jafc.5b05691>.
- (81) Waller, P. J.; Thamsborg, S. M. Nematode Control in “green” Ruminant Production Systems. *Trends Parasitol.* **2004**, *20* (10), 493–497. <https://doi.org/10.1016/j.pt.2004.07.012>.
- (82) Hoste, H.; Torres-Acosta, J. F. J.; Sandoval-Castro, C. A.; Mueller-Harvey, I.; Sotiraki, S.; Louvandini, H.; Thamsborg, S. M.; Terrill, T. H. Tannin Containing Legumes as a Model for Nutraceuticals against Digestive Parasites in Livestock. *Vet. Parasitol.* **2015**, *212*, 5–17. <https://doi.org/10.1016/j.vetpar.2015.06.026>.
- (83) Mueller-Harvey, I.; Bee, G.; Dohme-Meier, F.; Hoste, H.; Karonen, M.; Kölliker, R.; Lüscher, A.; Niderkorn, V.; Pellikaan, W. F.; Salminen, J.-P.; et al. Benefits of Condensed Tannins in Forage Legumes Fed to Ruminants: Importance of Structure, Concentration, and Diet Composition. *Crop Sci.* **2019**, *59* (3), 861–885. <https://doi.org/10.2135/cropsci2017.06.0369>.
- (84) Miller, J. E.; Kaplan, R. M.; Pugh, D. G. Chapter 6 - Internal Parasites. In *Sheep and Goat Medicine*; Pugh, D. G., Baird, A. N. B. T.-S. and G. M. (Second E., Eds.; W.B. Saunders: Saint Louis, 2012; pp 106–125. <https://doi.org/https://doi.org/10.1016/B978-1-4377-2353-3.10006-X>.
- (85) Bahuaud, D.; Martinez-Ortiz De Montellano, C.; Chauveau, S.; Prevot, F.; Torres-Acosta, F.; Fouraste, I.; Hoste, H. Effects of Four Tanniferous Plant Extracts on the *in Vitro* Exsheathment of Third-Stage Larvae of Parasitic Nematodes. *Parasitology* **2006**, *132* (4), 545–554. <https://doi.org/10.1017/S0031182005009509>.
- (86) Karonen, M.; Ahern, J. R.; Legroux, L.; Suvanto, J.; Engström, M. T.; Sinkkonen, J.; Salminen, J.; Hoste, H. Ellagitannins Inhibit the Exsheathment of *Haemonchus Contortus* and *Trichostrongylus Colubriformis* Larvae: The Efficiency Increases Together with the Molecular Size. *J. Agric. Food Chem.* **2020**, *68* (14), 4176–4186. <https://doi.org/10.1021/acs.jafc.9b06774>.
- (87) Spiegler, V.; Liebau, E.; Hensel, A. Medicinal Plant Extracts and Plant-Derived Polyphenols with Anthelmintic Activity against Intestinal Nematodes. *Nat. Prod. Rep.* **2017**, *34* (6), 627–643. <https://doi.org/10.1039/C6NP00126B>.
- (88) Novobilský, A.; Mueller-Harvey, I.; Thamsborg, S. M. Condensed Tannins Act against Cattle Nematodes. *Vet. Parasitol.* **2011**, *182* (2–4), 213–220. <https://doi.org/10.1016/j.vetpar.2011.06.003>.
- (89) Williams, A. R.; Fryganas, C.; Ramsay, A.; Mueller-Harvey, I.; Thamsborg, S. M. Direct Anthelmintic Effects of Condensed Tannins from Diverse Plant Sources against *Ascaris Suum*. *PLoS One* **2014**, *9* (5). <https://doi.org/10.1371/journal.pone.0097053>.

- (90) Naumann, H. D.; Armstrong, S. A.; Lambert, B. D.; Muir, J.-P.; Tedeschi, L. O.; Kothmann, M. M. Effect of Molecular Weight and Concentration of Legume Condensed Tannins on *in Vitro* Larval Migration Inhibition of *Haemonchus Contortus*. *Vet. Parasitol.* **2014**, *199* (1–2). <https://doi.org/10.1016/j.vetpar.2013.09.025>.
- (91) Whitney, T. R.; Lee, A. E.; Klein, D. R.; Scott, C. B.; Craig, T. M.; Muir, J.-P. A Modified *in Vitro* Larvae Migration Inhibition Assay Using Rumen Fluid to Evaluate *Haemonchus Contortus* Viability. *Vet. Parasitol.* **2011**, *176* (2–3), 217–225. <https://doi.org/10.1016/j.vetpar.2010.10.050>.
- (92) Rabel, B.; Mcgregor, R.; Douch, P. G. C. Improved Bioassay for Estimation of Inhibitory Effects of Ovine Gastrointestinal Mucus and Anthelmintics on Nematode Larval Migration. *Int. J. Parasitol.* **1994**, *24* (5), 671–676. [https://doi.org/10.1016/0020-7519\(94\)90119-8](https://doi.org/10.1016/0020-7519(94)90119-8).
- (93) Han, Q.; Eriksen, L.; Boes, J.; Nansen, P. Effects of Bile on the *in Vitro* Hatching, Exsheathment, and Migration of *Ascaris suum* Larvae. *Parasitol. Res.* **2000**, *86* (8), 630–633. <https://doi.org/10.1007/PL00008543>.
- (94) Peña-Espinoza, M.; Valente, A. H.; Bornancin, L.; Simonsen, H. T.; Thamsborg, S. M.; Williams, A. R.; López-Muñoz, R. Anthelmintic and Metabolomic Analyses of Chicory (*Cichorium intybus*) Identify an Industrial by-Product with Potent *in vitro* Antinematodal Activity. *Vet. Parasitol.* **2020**, *280*, 109088. <https://doi.org/10.1016/j.vetpar.2020.109088>.
- (95) Ramsay, A.; Williams, A. R.; Thamsborg, S. M.; Mueller-Harvey, I. Galloylated Proanthocyanidins from Shea (*Vitellaria paradoxa*) Meal Have Potent Anthelmintic Activity against *Ascaris suum*. *Phytochemistry* **2016**, *122*, 146–153. <https://doi.org/10.1016/j.phytochem.2015.12.005>.
- (96) Klongsiriwet, C.; Quijada, J.; Williams, A. R.; Mueller-Harvey, I.; Williamson, E. M.; Hoste, H. Synergistic Inhibition of *Haemonchus contortus* Exsheathment by Flavonoid Monomers and Condensed Tannins. *Int J Parasitol-Drug*, **2015**, *5*, 127–134. <https://doi.org/10.1016/j.ijpddr.2015.06.001>.
- (97) Desrues, O.; Fryganas, C.; Ropiak, H. M.; Mueller-Harvey, I.; Enemark, H. L.; Thamsborg, S. M. Impact of Chemical Structure of Flavanol Monomers and Condensed Tannins on *in vitro* Anthelmintic Activity against Bovine Nematodes. *Parasitology* **2016**, *143* (4), 444–454. <https://doi.org/10.1017/S0031182015001912>.
- (98) Quijada, J.; Fryganas, C.; Ropiak, H. M.; Ramsay, A.; Mueller-Harvey, I.; Hoste, H. Anthelmintic Activities against *Haemonchus Contortus* or *Trichostrongylus Colubriformis* from Small Ruminants Are Influenced by Structural Features of Condensed Tannins. *J. Agric. Food Chem.* **2015**, *63* (28), 6346–6354. <https://doi.org/10.1021/acs.jafc.5b00831>.
- (99) Brunet, S.; Hoste, H. Monomers of Condensed Tannins Affect the Larval Exsheathment of Parasitic Nematodes of Ruminants. *J. Agric. Food Chem.* **2006**, *54* (20), 7481–7487. <https://doi.org/10.1021/jf0610007>.
- (100) Molan, A. L.; Sivakumaran, S.; Spencer, P. A.; Meagher, L. P. Green Tea Flavan-3-Ols and Oligomeric Proanthocyanidins Inhibit the Motility of Infective Larvae of *Teladorsagia Circumcincta* and *Trichostrongylus Colubriformis* *in Vitro*. *Res. Vet. Sci.* **2004**, *77* (3), 239–243. <https://doi.org/10.1016/j.rvsc.2004.04.010>.
- (101) Girard, M.; Dohme-Meier, F.; Kragten, S.; Brinkhaus, A.; Arrigo, Y.; Wyss, U.; Bee, G. Modification of the Proportion of Extractable and Bound Condensed Tannins in Birdsfoot Trefoil (*Lotus Corniculatus*) and Sainfoin (*Onobrychis Viciifolia*) during Wilting, Ensiling and Pelleting Processes. *Biotechnol. Anim. Husb.* **2018**, *34* (1), 1–19. <https://doi.org/10.2298/bah1801001g>.
- (102) Lorenz, M. M.; Eriksson, T.; Udén, P. Effect of Wilting, Silage Additive, PEG Treatment and Tannin Content on the Distribution of N between Different Fractions after Ensiling of Three Different Sainfoin (*Onobrychis viciifolia*) Varieties. *Grass Forage Sci.* **2010**, *65* (2), 175–184. <https://doi.org/10.1111/j.1365-2494.2010.00736.x>.
- (103) Terrill, T. H.; Rowan, A. M.; Douglas, G. B.; Barry, T. N. Determination of Extractable and Bound Condensed Tannin Concentrations in Forage Plants, Protein Concentrate Meals and Cereal Grains. *J. Sci. Food Agric.* **1992**, *58* (3), 321–329. <https://doi.org/10.1002/jsfa.2740580306>.

- (104) Hellström, J. K.; Mattila, P. H. HPLC Determination of Extractable and Unextractable Proanthocyanidins in Plant Materials. *J. Agric. Food Chem.* **2008**, *56* (17), 7617–7624. <https://doi.org/10.1021/jf801336s>.
- (105) Malisch, C. S.; Lewandowski, L.; Salminen, J.-P.; Taube, F.; Lüscher, A. Low Concentrations of Protein- And Fiber-Bound Proanthocyanidins in Sainfoin (*Onobrychis viciifolia*) Are Stable across Accessions, Growth Stages, and Drought Conditions. *J. Agric. Food Chem.* **2020**, *68* (28), 7369–7377. <https://doi.org/10.1021/acs.jafc.0c01540>.
- (106) Minnee, E. M. K.; Woodward, S. L.; Waghom, G. C.; Laboyrie, P. G. The Effect of Ensiling Forage Legumes on Condensed Tannins. *Agronomy* **2002**, *32*, 117–119.
- (107) Kommu, D. S.; Barker, T.; Desai, S.; Burke, J. M.; Ramsay, A.; Mueller-Harvey, I.; Miller, J. E.; Mosjidis, J. A.; Kamiseti, N.; Terrill, T. H. Use of Pelleted Sericea Lespedeza (*Lespedeza Cuneata*) for Natural Control of Coccidia and Gastrointestinal Nematodes in Weaned Goats. *Vet. Parasitol.* **2014**, *204* (3–4), 191–198. <https://doi.org/10.1016/j.vetpar.2014.04.017>.
- (108) Ramsay, A.; Drake, C.; Grosse Brinkhaus, A.; Girard, M.; Copani, G.; Dohme-Meier, F.; Bee, G.; Niderkorn, V.; Mueller-Harvey, I. Sodium Hydroxide Enhances Extractability and Analysis of Proanthocyanidins in Ensiled Sainfoin (*Onobrychis Viciifolia*). *J. Agric. Food Chem.* **2015**, *63* (43), 9471–9479. <https://doi.org/10.1021/acs.jafc.5b04106>.
- (109) Quijada, J.; Drake, C.; Gaudin, E.; El-Korso, R.; Hoste, H.; Mueller-Harvey, I. Condensed Tannin Changes along the Digestive Tract in Lambs Fed with Sainfoin Pellets or Hazelnut Skins. *J. Agric. Food Chem.* **2018**, *66*, 2136–2142. <https://doi.org/10.1021/acs.jafc.7b05538>.
- (110) Desrues, O.; Mueller-Harvey, I.; Pellikaan, W. F.; Enemark, H. L.; Thamsborg, S. M. Condensed Tannins in the Gastrointestinal Tract of Cattle after Sainfoin (*Onobrychis Viciifolia*) Intake and Their Possible Relationship with Anthelmintic Effects. *J. Agric. Food Chem.* **2017**, *65* (7), 1420–1427. <https://doi.org/10.1021/acs.jafc.6b05830>.
- (111) Theodoridou, K. *The Effects of Condensed Tannins in Sainfoin ( Onobrychis viciifolia ) on Its Digestion and Nutritive Value*; Université Blaise Pascal - Clermont-Ferrand II, 2010.
- (112) Malisch, C. S.; Lüscher, A.; Baert, N.; Engström, M. T.; Studer, B.; Fryganas, C.; Suter, D.; Mueller-Harvey, I.; Salminen, J.-P. Large Variability of Proanthocyanidin Content and Composition in Sainfoin (*Onobrychis viciifolia*). *J. Agric. Food Chem.* **2015**, *63* (47), 10234–10242. <https://doi.org/10.1021/acs.jafc.5b04946>.
- (113) Oksanen, A.; Eriksen, L.; Roepstorff, A.; Ilsøe, B.; Nansen, P.; Lind, P. Embryonation and Infectivity of *Ascaris suum* Eggs. A Comparison of Eggs Collected from Worm Uteri with Eggs Isolated from Pig Faeces. *Acta Vet. Scand.* **1990**, *31* (4), 393–398.
- (114) R Core Team. *R: A Language and Environment for Statistical Computing*. R Foundation for Statistical Computing; Vienna, Austria, 2019.
- (115) RStudio, T. *RStudio: Integrated Development for R*. RStudio, Inc.; Boston, MA, 2019.
- (116) Wickham, H. *Ggplot2: Elegant Graphics for Data Analysis*; Springer-Verlag: New York, 2016.
- (117) Sanchez, G. *Plsdepot: Partial Least Squares (PLS) Data Analysis Methods*. **2012**.
- (118) Li, H. J.; Deinzer, M. L. Tandem Mass Spectrometry for Sequencing Proanthocyanidins. *Anal. Chem.* **2007**, *79* (4), 1739–1748. <https://doi.org/10.1021/ac061823v>.
- (119) Siebert, K. J. Effects of Protein-Polyphenol Interactions on Beverage Haze, Stabilization, and Analysis. *J. Agric. Food Chem.* **1999**, *47* (2), 353–362. <https://doi.org/10.1021/jf980703o>.
- (120) Salminen, J.-P. Two-Dimensional Tannin Fingerprints by Liquid Chromatography Tandem Mass Spectrometry Offer a New Dimension to Plant Tannin Analyses and Help To Visualize the Tannin Diversity in Plants. *J. Agric. Food Chem.* **2018**, *66* (35), 9162–9171. <https://doi.org/10.1021/acs.jafc.8b02115>.
- (121) Koupai-Abyazani, M. R.; McCallum, J.; Bohm, B. A. Identification of the Constituent Flavanoid Units in Sainfoin Proanthocyanidins by Reversed-Phase High-Performance Liquid Chromatography. *J. Chromatogr., A* **1992**, *594* (1–2), 117–123. [https://doi.org/10.1016/0021-9673\(92\)80319-P](https://doi.org/10.1016/0021-9673(92)80319-P).





UNIVERSITY  
OF TURKU

# STRUCTURE ELUCIDATION AND RUMINANT- RELATED BIOACTIVITIES OF PURIFIED PROANTHOCYANIDINS

---

Milla Leppä